CELL MIGRATION AND SURVIVAL PATHWAYS
IN CARDIAC DEVELOPMENT AND DISEASE

APPROVED BY SUPERVISORY COMMITTEE

Deepak Srivastava, M.D. (Mentor)

Jane Johnson, Ph.D. (Committee Chair)

Masashi Yanagisawa, M.D., Ph.D.

Helen Yin, Ph.D.

ACKNOWLEDGEMENTS

The research detailed herein would not have been possible without the collaboration and support, both in and out of the lab, of many individuals.

Within the lab, I first and foremost have to acknowledge my mentor Deepak, aka 'Bossman', for his consistent support, thoughtful insights, and patient steering of an impetuous graduate student's often random scientific impulses. Thank you, Deepak, for fostering a welcoming lab environment, for looking out for my interests, and for having the foresight to guide but never push. And to rebut the infamous insinuation of a postdoc in the lab, no, we do not just see you as a cash cow. Moo.

Ildi, thank you for a fruitful collaboration on the thymosin β4 project. An even bigger thank you for the years of conversation and insights more valuable than any scientific data. And thank you for bringing me awesome chicken soup when I was stuck in lab during the Christmas holidays. I'm definitely visiting you in Hungary just so you can feed me. Garrett, thanks for being a great baymate, a thoughtful scientist to talk shop with, and a constant source of interesting information and entertainment for the whole lab. Ildi has spread word of your omniscience to all corners of the globe, er, well, the lab. And Hungary.

To the rest of the lab, a big thanks for keeping work fun. Enjoying the company of one's coworkers is invaluable stimulus for waking up in the morning. Never mind that I never made it in until almost lunchtime…

Thank you Stephen Johnson for help over the years with issues both computer and non-computer-related. I value your friendship greatly and wish you the best of luck in life. May your daughter become a WNBA star and hook you up with courtside seats to NBA games. Trust me, I'm staying in touch with her, uh, I mean you.

For a stimulating collaboration, generous help with reagents and mice, and constant support throughout the years, thanks to Mark Henkemeyer and everyone in his lab.

I am grateful for the hard work of Michael D. White in J. Michael DiMaio's lab for endless coronary artery ligations and for a friendship that I hope will grow and strengthen over the years. I'll be living within walking distance of Fenway Park, so come on up for a Red Sox game anytime.

Thanks to the histology core run by Dr. Jim Richardson for sectioning, histology advice and protocols, venison jerky and stew, and accepting payment in beer.

Outside of the lab, I owe of course all of my success to my family, particularly my parents who sacrificed so much through the years to give their children every possible opportunity. Your support, unconditional love, and in particular your amazing homemade food have made it all possible.

Last but not least, a special thanks to a special lady in my life, Dr. Arwyn Hood, who went above and beyond the call of duty to become my unofficial lab tech at crunch time. A significant chunk of the data in Chapter Four literally would not have been possible without you. Thank you for that and more importantly, for your fiercely unwavering love. Brack.

Ok, I'm done now. Really. Seriously, is anyone reading this actually still awake? I know I'm not.

CELL MIGRATION AND SURVIVAL PATHWAYS IN CARDIAC DEVELOPMENT AND DISEASE

by

ANKUR SAXENA

DISSERTATION

Presented to the Faculty of the Graduate School of Biomedical Sciences

The University of Texas Southwestern Medical Center at Dallas

In Partial Fulfillment of the Requirements

For the Degree of

DOCTOR OF PHILOSOPHY

The University of Texas Southwestern Medical Center at Dallas

Dallas, Texas

August, 2005

CELL MIGRATION AND SURVIVAL PATHWAYS
IN CARDIAC DEVELOPMENT AND DISEASE

Publication No. _____

Ankur Saxena, Ph.D.

The University of Texas Southwestern Medical Center at Dallas, 2005

Supervising Professor: Deepak Srivastava, M.D.

Mammalian cardiac development is a complex process, rendering it susceptible to errors. As a result, congenital heart defects are the most common type of birth defect. Furthermore, heart disease in adults is the leading cause of mortality in the developed world. Given these statistics, gaining an understanding of cardiac development and disease is of paramount importance.

Here, data are presented suggesting that the signaling molecules SDF-1, ephrin-B1, and ephrin-B2 play important roles in proper valve formation and maturation during cardiogenesis. Furthermore, another signaling molecule, thymosin β4, is implicated in promoting cell survival, potentially through an ILK-Akt pathway, as well as angiogenesis in

the treatment of mice post-myocardial infarction. Finally, SDF-1 not only plays a role in cardiac development but, in a manner strikingly similar to the actions of thymosin β4, also appears to have therapeutic benefit post-myocardial infarction through the ILK-Akt pathway, reduced cell death, and increased angiogenesis. Together, these data and other information presented herein suggest new roles for signaling molecules in both cardiogenesis and cardiac therapy.

TABLE OF CONTENTS

PUBLICATIONS

Saxena A, White MD, DiMaio JM, Srivastava D. Stromal cell-derived factor-1 alpha promotes cardiomyocyte survival and cardiac repair post-infarction. *In Preparation*

Saxena A & Srivastava D. SDF-1α and ephrin-B1 guide endothelial cell migration during valvulogenesis. *In Preparation.*

Gao J[*], Lee K[*], Zhao M, Qiu J, Zhan X, **Saxena A**, Moore CJ, Cohen SN, Georgiou G. Differential Modulation of *E. coli* mRNA Abundance by Protein Inhibitors of RNase E Activity. ***Proc. Natl. Acad. Sci., USA***, *Submitted.*

Bock-Marquette I[*], **Saxena A**[*], White MD, DiMaio JM, Srivastava D. Thymosin β4 activates integrin-linked kinase and promotes cardiac cell migration, survival and cardiac repair. ***Nature*** (article), 432(7016), 466-72 (2004).

Cowan CA[*], Yokoyama N[*], **Saxena A**, Chumley MJ, Silvany RE, Baker LA, Srivastava D, Henkemeyer M. Ephrin-B2 reverse signaling is required for axon pathfinding and cardiac valve formation but not early vascular development. ***Developmental Biology***, 271(2), 263-71 (2004).

* These authors contributed equally.

LIST OF FIGURES

CHAPTER ONE: INTRODUCTION

CHAPTER TWO: ROLES OF SDF-1, EPHRIN-B1, AND EPHRIN-B2 IN VALVULOGENESIS

CHAPTER THREE: THYMOSIN β4 PARTIALLY RESCUES MYOCARDIAL DAMAGE POST-INFARCTION

CHAPTER FOUR: SDF-1 PARTIALLY RESCUES MYOCARDIAL DAMAGE POST-INFARCTION

ABBREVIATIONS AND DEFINITIONS

Allogenic –Same species, different genetic makeup

Angiogenesis – Sprouting of new microvasculature from existing vessels

Beer – an alcoholic beverage normally comprising ~ 25% of a graduate student's blood

BMP – bone morphogenetic protein

CHD – congenital heart defect

CXCR4 – G-protein coupled receptor for the chemokine SDF-1

DNA – deoxyribonucleic acid

E10.0 – Embryonic day of development, here referring to mouse gestation day 10

Echocardiography – Noninvasive ultrasound imaging of the heart to study structure and function

ECM – extracellular matrix

EDD – end diastolic dimension, i.e. the maximum diameter of a ventricle (relaxed)

EDV – end diastolic volume, i.e. the maximum amount of blood in a ventricle (relaxed)

Ejection fraction (%) – two-dimensional area measurement (the derivative) of three-dimensional blood flow, i.e. the fraction of blood ejected from the left ventricle with each contraction; EF (%) = (EDV-ESV)/EDV * 100

EMT – epithelial-mesenchymal transformation

Endocardium – interior lining of the heart in direct contact with the blood inside

Ephrins/Eph receptors – cell surface signaling molecules usually mediating cell repulsion

ESD – end systolic dimension, i.e. the minimum diameter of a ventricle (contracted)

ESV – end systolic volume, i.e. the minimum amount of blood in a ventricle (contracted)

Fractional shortening – one-dimensional line measurement (the derivative) of two-dimensional wall movement; FS (%) = (EDD-ESD)/EDD * 100

Hypoxia – deprivation of oxygen

Intracardiac – here, referring to injection into the muscle of the heart

Intraperitoneal – within the peritoneal cavity (a type of systemic administration)

Ischemia – deprivation of blood supply

Ligation (of artery) – Suturing off of the artery to block blood flow to downstream tissue

Mitral Valve – atrioventricular valve leading from the left atrium to the left ventricle

Murine – in/of the mouse

Myocardial infarction – heart attack

Myocardium – heart muscle tissue

P_0 – postnatal day 0 (day of birth)

PBS – phosphate buffered saline

RNA – ribonucleic acid

SDF-1α – stromal cell-derived factor-1 alpha, referred to in the text as SDF-1

Semilunar Valve – an outflow tract valve, i.e. aortic or pulmonary

Stenosis – constriction or narrowing

Tricuspid Valve – atrioventricular valve leading from the right atrium to the right ventricle

Tβ4 – thymosin β4

CHAPTER ONE
Introduction

CARDIAC DEVELOPMENT & DISEASE

Cardiac Development

Mammalian cardiac development is a precisely defined amalgam of cellular proliferation, migration, differentiation, and death. The heart is the first organ to form, with mesoderm progenitor cells assembling to form the cardiac crescent. These cells then join at the midline to establish a linear heart tube which undergoes rightward looping to properly position the future chambers of the heart. Finally, morphogenesis of this structure creates a mature, four-chambered heart (Fig.1a). Mistakes in this complex process comprise the most common type of defect in newborns, with approximately 1% of all such abnormalities classified as congenital heart defects (CHDs) (Olson & Srivastava, 1996). Furthermore, 25% to 30% of these are valve-related defects (Loffredo, 2000), a statistic that highlights the importance of elucidating the mechanisms of valvulogenesis.

The first step of valve development begins as the linear heart tube loops and then repositions to correctly orient the organ. At this time, as early as approximately E10.0 in the mouse, epithelial-mesenchymal transformation (EMT) of endothelial cells in response to signaling from adjacent myocardium occurs. This signaling cascade is thought to include members of the TGF-β signaling family such as BMP-2 (Yamagishi et al., 1999; Sugi et al., 2004), BMP-6, and BMP-7 (Kim et al., 2001) ; however, the end mediators of such a cascade that directly signal endothelial cells to move, stop, and change direction are unknown. In

between the myocardium and endocardium lies an acellular cardiac jelly, also known as the extracellular matrix (ECM), which consists primarily of collagen prior to EMT. Transforming cells lose their endothelial profile in lieu of mesenchymal morphology as they invade into this ECM, producing the first precursor of cushion tissue (Markwald et al., 1977; Fig. 1b). Later in development, myocardial cells from the inner curvature of the looping heart tube invade a portion of the mesenchyme, as do some neural crest cells and epicardial cells from the pro-epicardial organ. Subsequent stages of valvular development up until birth and slightly beyond include substantial loss of tissue to properly shape the valves, the mechanism of which is largely unknown. By the time of birth, an initially bulbous mass of mostly mesenchymal cells has transformed into a thin leaflet that is capable of regulating blood flow through the heart.

While many upstream components of regulatory pathways have been elucidated that ostensibly direct cellular movement, little is known about the downstream effector molecules that directly tell the cells to migrate. Work outlined herein sheds some light on particular ligands and receptors that may be key players in migration both during cardiogenesis and in treatment of adult cardiac disease.

Cardiac Disease

Problems encountered in the heart at or before birth are certainly not the only cause for concern. Heart disease has for many decades been the number one killer of adults in the industrialized world (Braunwald, 1997; Jessup & Brozena, 2003). A large segment of this affliction is due to coronary artery disease reducing or eliminating blood flow to an area of the heart; statistics from the American Heart Association show that in 2002, over seven

million Americans were victims of myocardial infarctions, or heart attacks, as a result of this phenomenon.

Most patients having had a heart attack arrive at a medical care facility post-infarction. Current methods of treatment in this situation rely predominantly on (a) stabilizing the patient and allowing gradual partial healing to take place in the heart and (b) supplementing this recovery with drugs such as thiozides, beta blockers, and ace inhibitors that are thought to reduce detrimental remodeling of the heart and/or reduce myocardial oxygen demand (Jessup & Brozena, 2003; personal communication, Arwyn E. Hood, M.D., Emergency Medicine, 2005). However, such methodology can essentially be thought of as damage control, and the emergency medicine physician has no practical options to slow or prevent the immediate expansion of the damaged area (see Fig. 2). The presence of easily administrable compounds such as recombinant proteins, absent of the danger of immunorejection that exists with allogenic cells, would be a significant addition to a physician's arsenal.

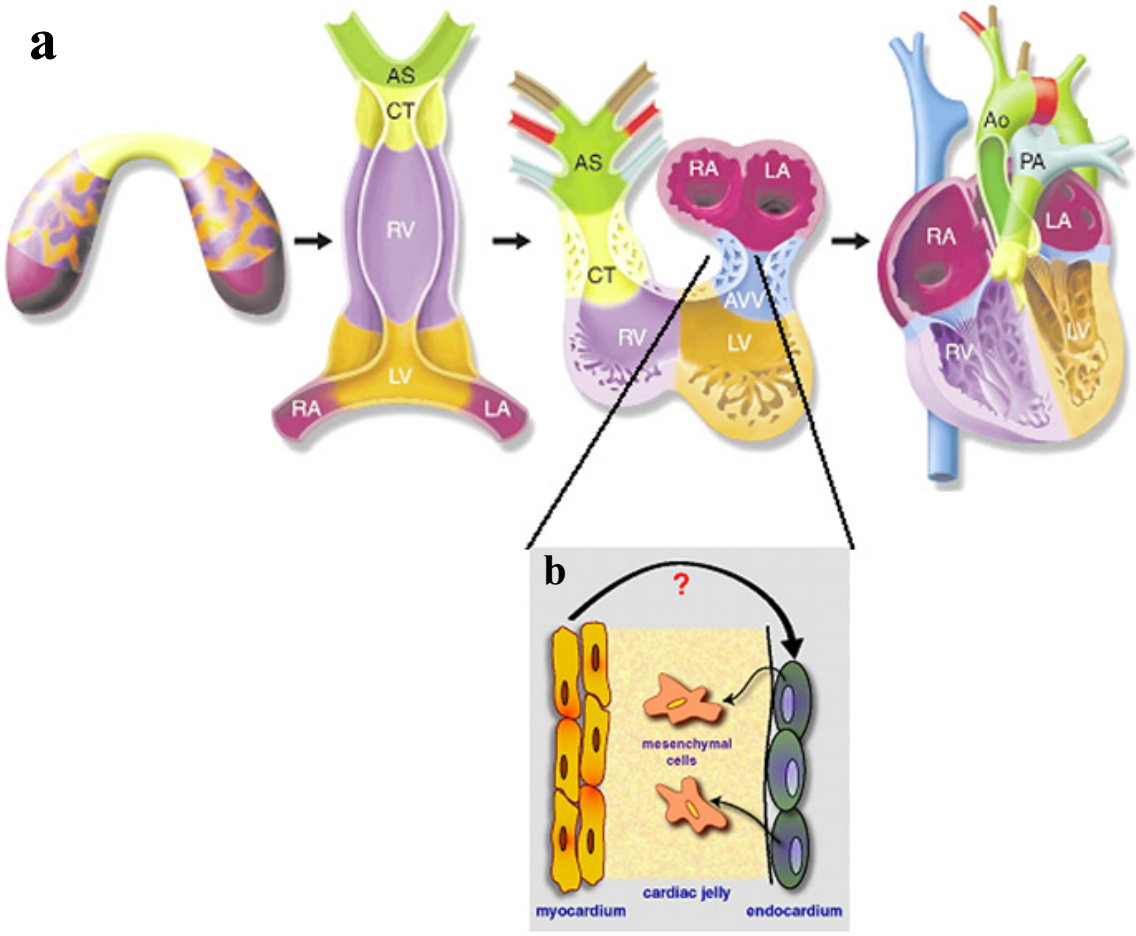

Figure 1-1. Schematic of mammalian cardiogenesis. (a) The early cardiac crescent fuses to form a linear heart tube which then loops to the right. Cell proliferation, differentiation, death, and migration fuel morphogenesis into the mature, 4-chambered heart. (Adapted from Srivastava & Olson, 2000) **(b)** Epithelial-mesenchymal transformation (EMT) results in invasion of cells into initially acellular cardiac jelly to form cushion tissue in both the conotruncal (CT) and atrioventricular valve (AVV) regions. This is thought to occur in response to signals from the myocardium that may include members of the BMP signaling family. (Illustration courtesy of Aparna Aiyer) Ao, aorta; LA, left atrium; LV, left ventricle; PA, pulmonary artery; RA, right atrium; RV, right ventricle.

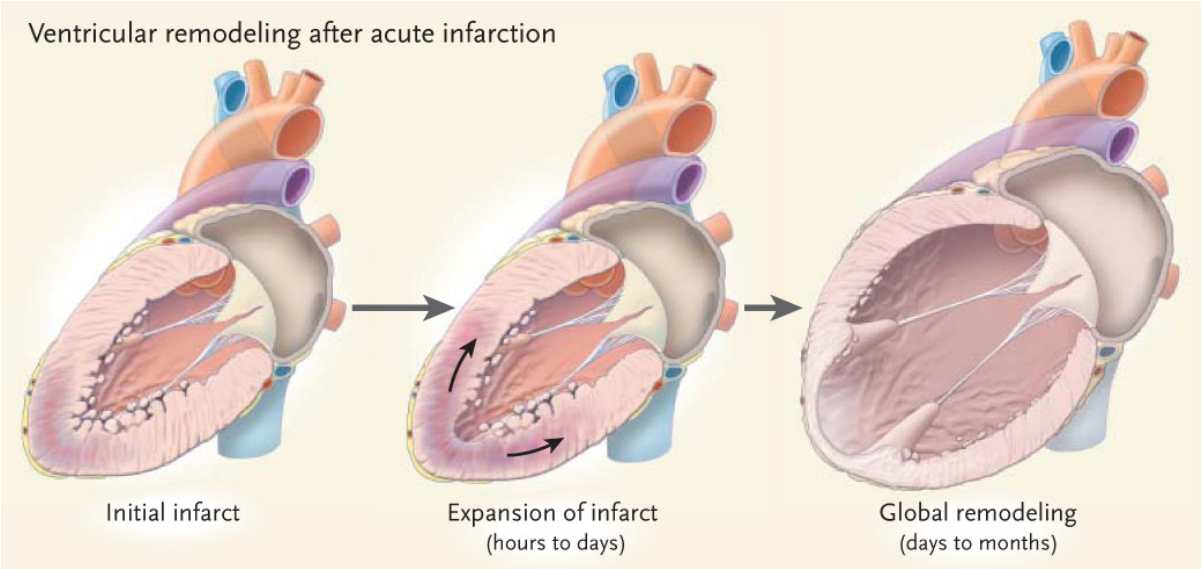

Figure 1-2. Cardiac disease timeline post-infarction. In a matter of hours or days after a heart attack, damage begins to spread to surrounding myocardium that is inadequately supplied with blood. Eventually, detrimental global remodeling occurs as the heart attempts to compensate for decreased function, resulting in cardiac dilation and mitral valve dysfunction, among other problems. (Adapted from Jessup & Brozena, 2003)

CHAPTER TWO

ROLES OF SDF-1, EPHRIN-B1, AND EPHRIN-B2 IN VALVULOGENESIS

Introduction

Among the numerous molecules involved in cardiogenesis are the secreted chemokine stromal cell-derived factor-1 (SDF-1) and its G-protein coupled receptor CXCR4. SDF-1α precursor protein is an 89 amino acid variant (the alternatively spliced SDF-1β has 4 more amino acids at its C-terminus). Experiments detailed in this dissertation all refer to SDF-1α, hereafter denoted as SDF-1.

SDF-1 signaling through CXCR4 most often stimulates a chemotactic response resulting in migration towards an increasing SDF-1 gradient (Bleul et al., 1996; Aiuti et al., 1997; Corcione et al., 2000; Doitsidou et al., 2002 and others). In addition, in some cell types such signaling can stimulate cell proliferation (Bajetto et al., 2001; Porcile et al., 2005 and others), survival (Zou et al., 2001; Kortesidis et al., 2005 and others), and angiogenesis (Mirshahi et al., 2000; Orimo et al., 2005 and others). Targeted deletions of the ligand and its receptor in mice show identical phenotypes, suggesting a monogamous relationship. These mice illustrate numerous defects including difficulties with hematopoiesis, lymphopoiesis, and decreased vascularization of the gastrointestinal tract; in addition, a highly penetrant ventricular septal defect (VSD) is observed. The vast majority of SDF-1 and CXCR4 null mouse embryos are embryonic lethal, with approximately 50% lethality by E17.5 and a small subset surviving until a few hours after birth (Nagasawa et al., 1996; Tachibana et al., 1998;

Zou et al., 1998). However, the mechanisms underlying the cardiovascular defects are unknown.

Given the paucity of information regarding the cardiac defects in SDF-1 and CXCR4-deficient mice, I undertook an extensive study of the heart, outflow vessels, and aortic arches in these animals to determine other potential defects. The hypothesis underlying this pursuit was based on the lethality observed. One possible reason for lethality in this knockout is a general systemic failure due to lack of SDF-1 signaling throughout the embryo. Alternatively, lethality may be due to cardiac or vascular abnormalities such as defects in septum formation, aortic arch arteries, valves, or in the outflow tract. To characterize such potential defects, techniques I used included injections with a polymerizing plastic to produce 3-dimensional casts of the aortic arch arteries, sectioning of embryos to compare histology to wild-type littermates, and gross examination of embryos to visually observe differences in development. In addition, CXCR4 +/- mice were crossed with Tie-2-LacZ mice to allow X-gal staining of vascular endothelium for easier visualization and were also crossed with SDF-1 +/- mice to study double homozygotes. While this search turned up mostly negative, it did establish that SDF-1 -/-; CXCR4 -/- double homozygotes had no apparent additional defects. This finding lends further weight to the idea that SDF-1 is the only ligand for CXCR4 and CXCR4 the only receptor for SDF-1, unusual among chemokines. In addition, this line of investigation led me onto a related examination of atrioventricular valve development, detailed in the results section.

In situ hybridization studies by McGrath, et al. of RNA expression patterns during embryonic development show widespread, complementary expression of the ligand and

receptor from approximately E7.5 to E12.5 in mice (1999). Most commonly, expression of SDF-1 is observed in mesenchymal or myocardial tissue while CXCR4 is expressed in adjacent endothelium or epithelium, with several exceptions. While expression is widespread, it is strictly regulated both temporally and spatially.

More specifically, in the heart and vasculature, I observed SDF-1 expression at various timepoints in several places including the myocardium of the inner curvature of the looping heart tube, mesenchyme of the outflow tract, the muscular portion of the interventricular septum, mesenchyme surrounding the developing aortic sac, myocardial trabeculations of the ventricles, and interstitial mesenchyme surrounding a subset of developing blood vessels including aortic arch arteries. CXCR4 was expressed in the aortopulmonary septum, endothelium of the outflow tract, atrioventricular valve tissue, and endothelium of developing blood vessels, amongst other places (data not shown).

Putative intracellular interactions between G proteins downstream of CXCR4 and the intracellular domain of ephrin-B1 have been suggested to regulate cell migration in cerebellar granule cells during development of the brain (Fig. 1; Lu et al., 2001). B-class ephrins and their Eph receptors comprise a subfamily of bi-directional, tyrosine kinase-mediated signaling molecules that generally act as mediators of cellular repulsion (reviewed in Schmucker & Zipursky, 2001; Palmer & Klein, 2003). I hypothesized that CXCR4 and ephrins may regulate cell migration during cardiac development analogous to that in the cerebellum. In addition, ephrin-B2, highly homologous to ephrin-B1, is expressed widely in the heart at later stages of cardiogenesis, leading me to investigate the role of this molecule as well in cardiac maturation.

Results

CXCR4 and ephrin-B1 Direct Cell Migration During EMT

Investigating the idea that CXCR4 and ephrin-B1 may cooperate intracellularly to regulate cell migration during cardiogenesis unfortunately proved difficult to elucidate. Experiments I attempted with subcellular immunocytochemistry, calcium flux signaling, and other methodology to establish a direct connection proved technically difficult or were inconclusive. However, this line of experimentation did nonetheless lead to some interesting results regarding valve development.

I used radioactive RNA in situ hybridization to establish that CXCR4 and ephrin-B1 were co-expressed during early valve cushion formation in murine embryos. This coexpression was spatiotemporally very specific, with almost no expression of either molecule at E10.5, very strong coexpression at E11.5, and fading expression by E12.5 (Fig. 2). There was no significant expression of ephrin-B2 in the AV valves (data not shown). As the CXCR4 and ephrin-B1 expression profiles corresponded well with the known timeframe of epithelial-mesenchymal transformation (EMT), I decided to study the effect of these molecules on EMT. In vitro collagen gel assays were employed that have been extensively used in the field to study valve formation (Bernanke & Markwald, 1982; Runyan & Markwald, 1983; Wunsch et al., 1994; van den Hoff et al, 1999; Fig. 3). Data from experiments with AV canal tissue harvested at E10.5 and placed on collagen gels suggested that ephrin-B1 placed in the collagen could affect EMT by inhibiting cellular migration in valve-forming tissue (Fig. 4). Blocking antibody against CXCR4 similarly inhibited cell migration (data not shown).

However, I remained concerned about using this experimental system whereby a cell entering the collagen gel would be surrounded by any added protein in equal concentrations on all sides once it entered the gel. Such an equimolar protein concentration was limited in its relevance to the in vivo situation where, for example, increasing concentrations of SDF-1 attract cells along that protein gradient. To better model the in vivo environment, I devised a protocol with beads normally used in binding columns for proteins. After proper equilibration, I incubated these beads with my proteins of interest such as SDF-1 and ephrin-B1. When the beads were placed in polymerizing gels to which explants were then added (see Methods section for further details), I observed that transforming mesenchymal cells, easily discernable by altered morphology and migration into the collagen gel, migrated towards SDF-1-soaked beads and away from ephrin-B1-soaked beads (Fig. 5).

The Cytoplasmic Domain of EphrinB2 is Required for Proper Valvulogenesis

While the in vivo function of ephrin-B1 in cardiogenesis is unknown, ephrin-B2, highly homologous to ephrin-B1, is expressed widely in the developing heart. Ephrin-B2-LacZ mice created in Mark Henkemeyer's lab at UT Southwestern have had the intracellular signaling region replaced with a LacZ domain and exhibit functional forward signaling but inoperative reverse signaling (Fig. 6). While mice completely lacking ephrin-B2 show embryonic lethality by E11.0 (Wang et al., 1998), as do mice with truncated ephrin-B2 lacking the intracellular signaling region (Adams et al., 2001), ephrin-B2-LacZ mice survive much longer, allowing analysis of late cardiac development. The Mendelian ratio of ephrin-B2-LacZ homozygous null embryos to wild-type littermates begins to decrease in late embryogenesis and homozygous nulls that make it to birth die within a few hours.

Looking at ephrin-B2 expression in late embryogenesis, I observed LacZ staining in ephrin-B2-LacZ heterozygote embryos and RNA in situ hybridization in wild-type embryos establishing strong ephrin-B2 expression in the endothelial layer of maturing valve leaflets (Fig. 7). I found that ephrin-B2-LacZ homozygous null embryos harvested at E18.5 and pups at P_0 (right after birth) demonstrated defects in proper formation of cardiac valve leaflets. Both the aortic and pulmonary valve leaflets were grossly enlarged and bulbous in comparison to wild-type littermates, and quantitation revealed over twice the normal number of cells (Fig. 8; Cowan & Yokoyama et al., 2004). Immunofluorescent staining showed normal amounts and placement of both collagen and myocardium in the mature valves and related structures (data not shown). Histological studies of the outflow tract valves revealed that at E12.5, when the addition of cells to cushion tissue was ending and leaflet maturation was beginning, homozygous-null cushions appeared identical to those from wild-type hearts. Further analysis of later timepoints suggested a developmental defect just prior to birth; however, the exact time of malformation could not be pinpointed (Fig. 9 & data not shown).

In addition to the outflow tract defects, I found that the tricuspid valve leaflet originating from the ventricular septum appears bulbous in nature and does not extend out from the underlying septum as far as in wild-type littermates. The mitral valve leaflets appear slightly thickened as well, although the extent of this phenotype is not nearly as severe as that of the semilunar leaflets (Fig. 10).

Cumulatively, these data demonstrate a previously unresolved role for ephrinB2-mediated reverse signaling in valve formation during cardiogenesis. Furthermore, the lethality observed in these mice within hours of birth may be explained at least in part by the

cardiac defects described herein. Thickened valves can restrict blood flow to an extent that renders the young pup unable to survive outside of the womb. Such thickened leaflets are a common, often lethal birth defect in humans.

Together, these studies suggest previously unknown roles for SDF-1, CXCR4, and ephrin-B1 in early valve cushion formation and for reverse signaling through ephrin-B2 in valve leaflet maturation. Further studies are in progress to establish an in vivo role for SDF-1 in cushion formation through creation of a transgenic mouse overexpressing SDF-1 specifically in the endocardium.

Discussion

While I have demonstrated in vitro the ability of SDF-1 and ephrin-B1 to guide endocardial cell migration, there is as yet no in vivo evidence to complement these findings. To this end, I am in the process of creating a transgenic mouse where SDF-1 expression is driven by the endocardial-specific enhancer segments of NFATc1. The purpose herein is to misexpress SDF-1 in endocardial cells which normally express CXCR4 but not SDF-1, thereby nullifying the endogenous chemotactic gradient necessary for directed endocardial cell migration and keeping the cells in their initial locations. My hypothesis is that such a disruption will result in histological defects in the cardiac valves not seen in the SDF-1 and CXCR4 knockout models where other signaling molecules may be able to compensate. Attempts to create this construct have so far been unsuccessful but are continuing.

The ephrin-B2 homozygous-null heart has been described to have defects in myocardial trabeculation formation, but further cardiac studies at later timepoints have not been possible due to the early lethality at E11.0 (Wang et al., 1998). The ephrinB2-LacZ

mice described here have allowed observation of cardiac development beyond this stage of embryogenesis. Thus, I have been able to pinpoint a previously unobserved role for ephrinB2-mediated reverse signaling in the development of cardiac valves.

Given the previous evidence for ephrins as guidance molecules involved in both repulsion and attraction, the thickened valves observed in the ephrinB2-LZ mice could be indicative of a role for reverse signaling through ephrins in (i) proliferation of mesenchymal cells (ii) apoptosis of cushion cells at later stages (iii) proper migration of invading cells and positioning of these cells and/or (iv) secretion of ECM (extracellular matrix) components between the cells. Unfortunately, a series of experiments done to investigate the above possibilities failed to pinpoint the exact cause, although the increased number of cells suggested that the over-secretion of ECM components was not the primary culprit. The vast number of timepoints between E12.5, when the wild-type and mutant valve precursors look identical, and birth, by which defects are observed, leaves a number of timepoints in need of thorough investigation to determine when and why the valve defects occur. While the low fertility rates of the ephrin-B2-LacZ mice made such studies an arduous task, it will hopefully be pursued in the future.

The importance of reverse signaling through ephrin-B2 during valve leaflet maturation has been established with the data from the ephrin-B2-LacZ mice. The most obvious unresolved question then is whether or not forward signaling through ephrin-B2 also plays a role in valve development or maturation. The ephrin-B2-LacZ mice were created to have LoxP sites flanking the LacZ portion. Crossing these mice with a Cre mouse allows creation of a truncated ephrin-B2 protein (ephrin-$B2^{T}$) that has been shown to be deficient in

both forward and reverse signaling and embryonically lethal prior to valvulogenesis (Adams et al., 2001). I have attempted crossing ephrin-B2-LacZ mice with NFATc1-driven Cre mice to create an endocardial-specific ephrin-$B2^{T}$, allowing analysis of valvulogenesis in the context of no ephrin-B2 signaling. These breeding attempts are continuing in the lab.

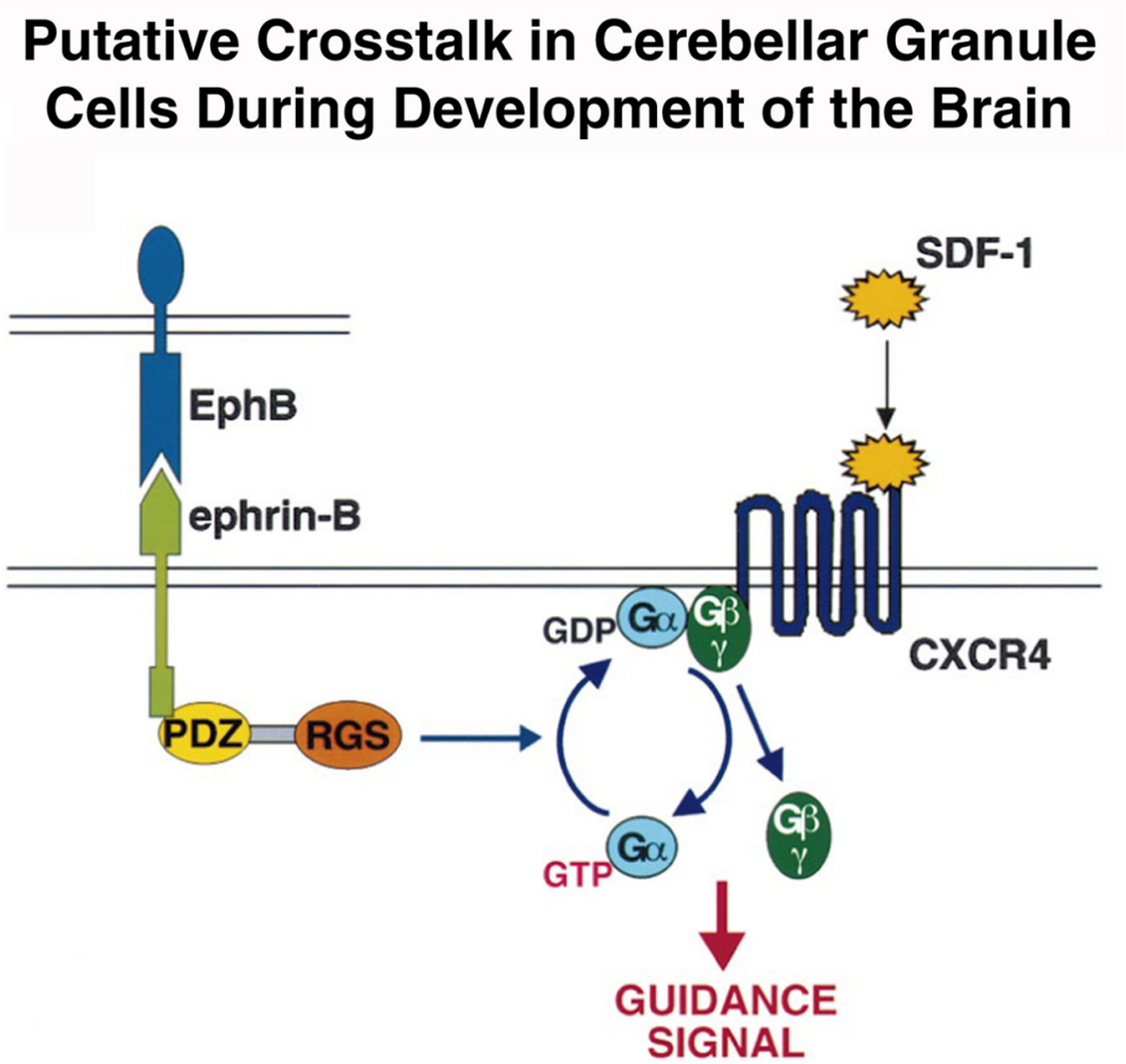

Figure 2-1. Model for crosstalk between CXCR4 & ephrins. Binding of B ephrins and their EphB receptors results in bidirectional signaling. Heterotrimeric G protein signaling is activated by ligands that act through seven-transmembrane receptors, such as the chemoattractant SDF-1 and its receptor CXCR4. PDZ-RGS3 binds the cytoplasmic C terminus of B ephrins through its PDZ domain, and inhibits heterotrimeric G protein signaling through the GAP activity of its RGS domain. (Adapted from Lu, et al, 2001)

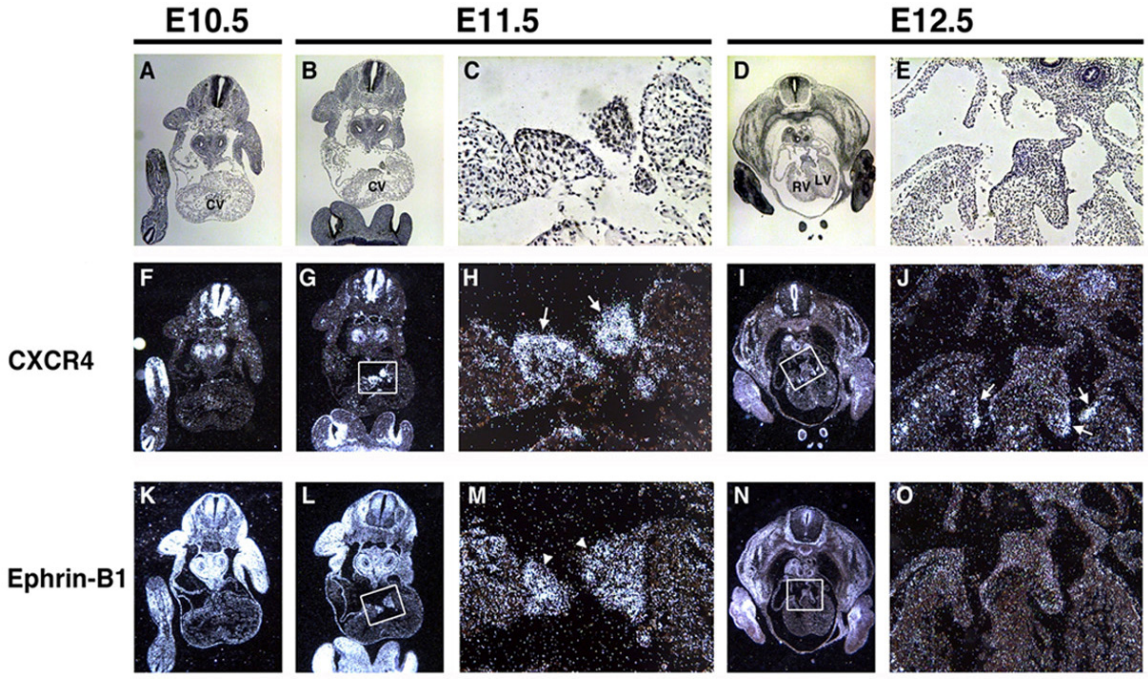

Figure 2-2. In situ hybridization of CXCR4 & ephrin-B1. Wild-type embryos were sectioned in a 4-chambered, transverse orientation, and adjacent sections were hybridized with probes for CXCR4 and ephrin-B1 at E10.5-12.5. Brightfield pictures **(A-E)** are shown for reference. While both genes demonstrate widespread expression, endocardial cushion tissue shows concurrent, upregulated expression of CXCR4 **(G-H)** (arrows) and ephrin-B1 **(L-M)** (arrowheads) at E11.5. Expression is faint at E10.5 **(F, K)** and fades by E12.5 **(I-J, N-O)**. Some CXCR4 expression remains in a subset of valvular tissue **(J)** (arrows).
(A-B, F-G, K-L) are shown at 4x magnification; **(C, H, M)** at 20x; **(D, I, N)** at 2.5x; **(E, J, O)** at 10x.
CV = Common Ventricle; LV = Left Ventricle; RV = Right Ventricle

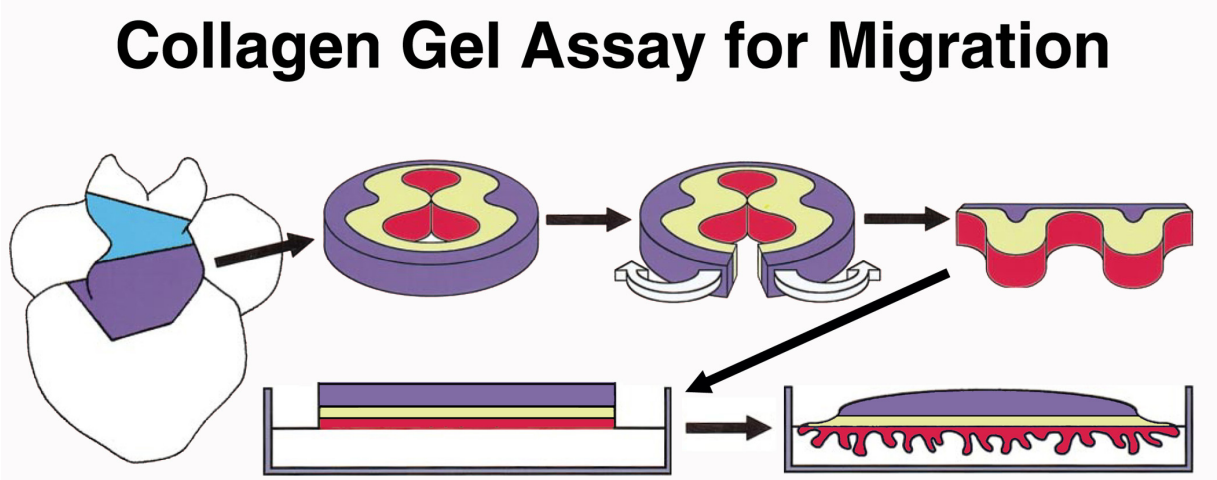

Figure 2-3. Collagen gel assay for migration. The region of interest, in this diagram the proximal portion of the outflow tract, is cut out, sliced open, and laid flat with the endothelial surface (red) facing down on a 3-dimensional collagen gel. Signaling thought to originate from the myocardium (purple) induces epithelial-mesenchymal transformation (EMT) of endocardial cells that then invade the collagen as mesenchymal cells. The yellow layer indicates the extracellular matrix that normally receives the invading cells in vivo. (Adapted from van den Hoff et al., 1999)

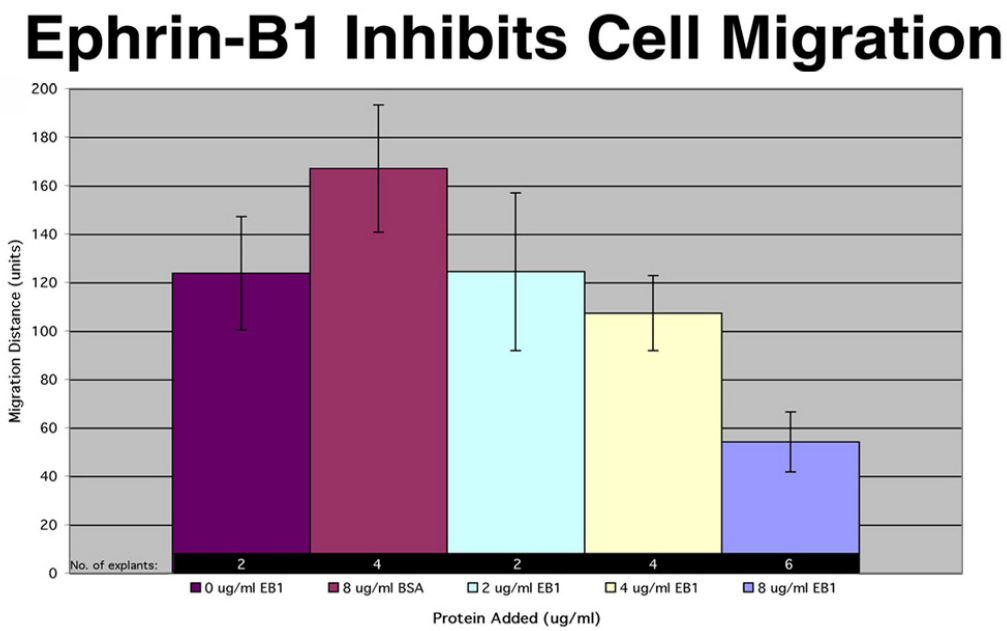

Figure 2-4. Ephrin-B1 inhibits cell migration. Explants of AVC tissue were sliced open at E10.5 and E11.5 and laid flat on a collagen gel to assay EMT and resulting migration into the gel. Significant migration is seen in the absence of any protein supplement in the gel. This can be compared to explants where 8 ug/ml bovine serum albumin (BSA) is added to the gel as a control and to explants where 2 ug/ml, 4ug/ml, or 8 ug/ml ephrin-B1 (EB1) is added. 8 ug/ml of ephrin-B1 significantly inhibits the degree of migration in comparison to 8 ug/ml of BSA. 8 measurements of migration distance were taken per explant at angle increments of 45°. This experiment has been repeated in triplicate. Numbers below each bar indicate the number of explants in each data series. Bars indicate 95% confidence limits. *$P < .001$ vs. 0 ug/ml EB1 and 8 ug/ml of BSA.

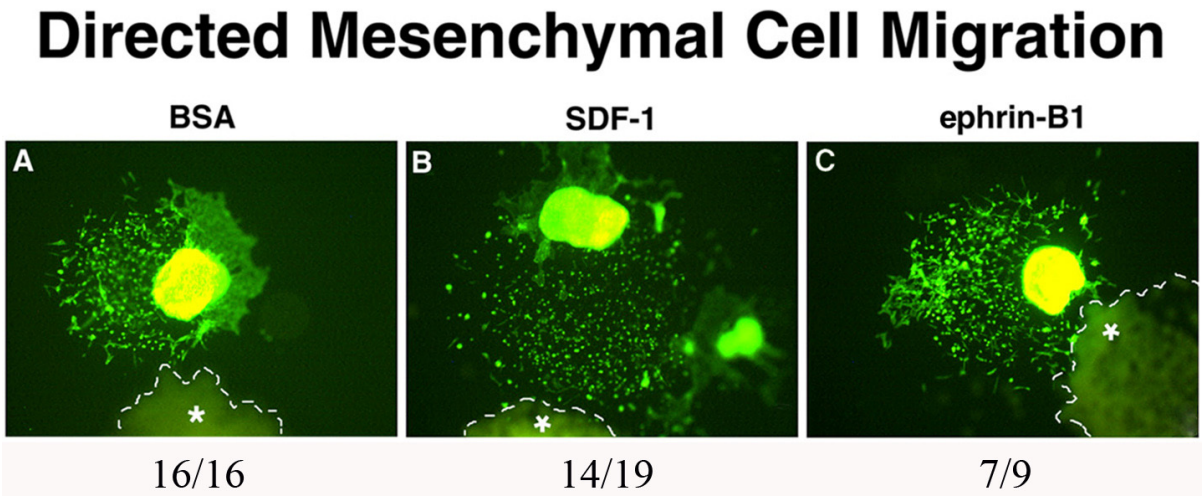

Figure 2-5. Directed mesenchymal cell migration. Protein-binding beads were soaked for 1 hour at RT with proteins of interest after equilibration at the proper relevant pH. Beads were spotted in polymerizing collagen gels used for the EMT assay described above. AVC explants at E10.5 were placed near the beads. Shown are examples of migration observed ~ 42 hours post-explantation that have been stained with actin-binding phalloidin to visualize the cells. Asterisks indicate the beads, encircled with dashed lines, in each picture. Migration in response to bovine serum albumin (BSA) occurs neither towards nor away from the beads **(A)**. In contrast, mesenchymal cells are seen migrating directly towards beads soaked in SDF-1α **(B)** and directly away from beads soaked in ephrin-B1 **(C)**. Numbers below indicate the total sum of scored explants for each protein. 16 of 16 explants (100%) migrated in other directions when placed next to BSA, 14 of 19 explants, or 74%, showed migration towards SDF-1α, and 7 of 9 explants, or 78%, migrated away from ephrin-B1.

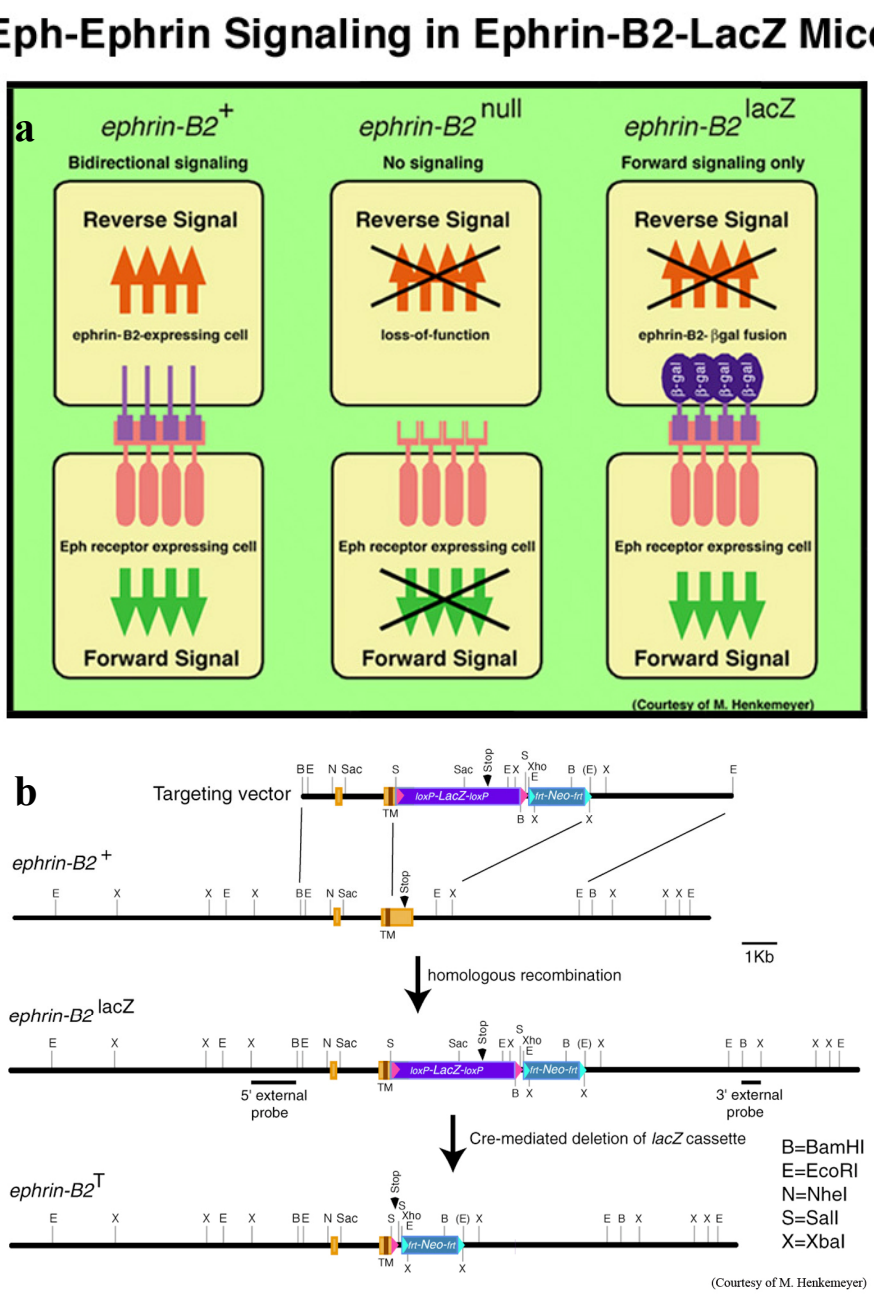

Figure 2-6. Eph-ephrin signaling in ephrin-B2-LacZ mice. (**a**) While wild-type mice **(left)** have proper bi-directional signaling, ephrin-B2 -/- mice **(center)** have no signaling. Ephrin-B2-LacZ mice **(right)** lack the intracellular domain of ephrin-B2, which has been replaced by a LacZ domain. The resulting fusion protein allows for proper forward signaling but no reverse signaling. (Figure courtesy of M. Henkemeyer) (**b**) Targeted deletion strategy for the ephrin-B2-LacZ mice made in Mark Henkemeyer's lab. Note the loxP sites surrounding the LacZ domain that allow for Cre-mediated ephrin-B2^{T} mice to be created.

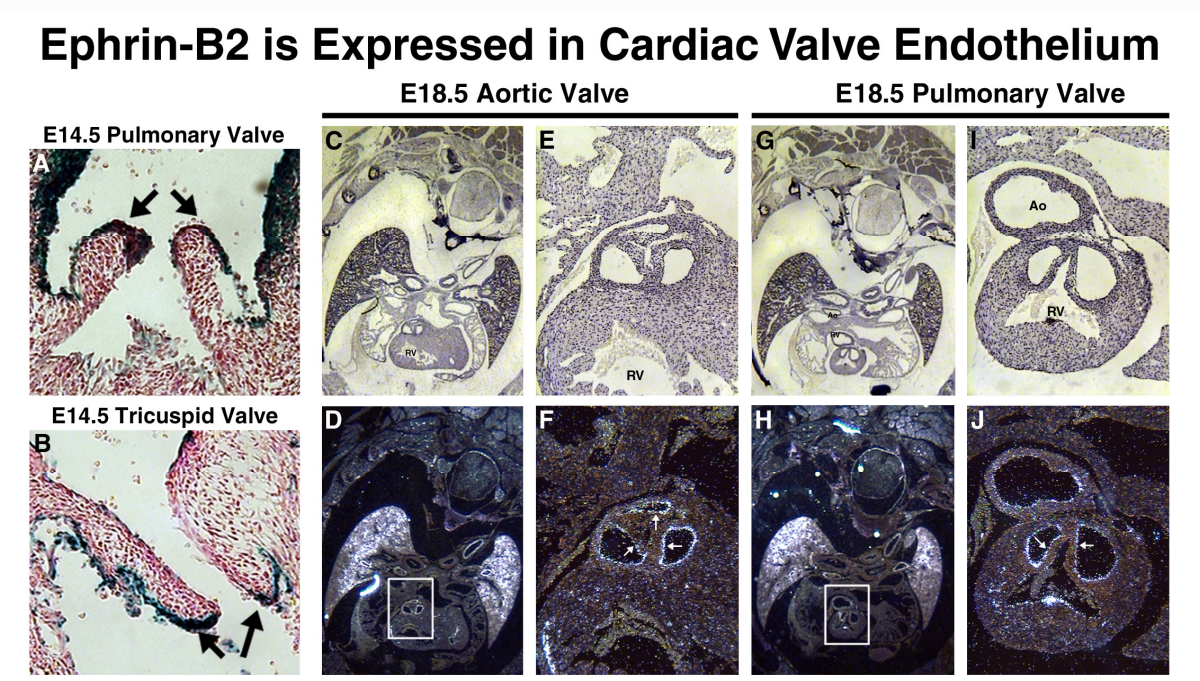

Figure 2-7. Ephrin-B2 is expressed in cardiac valve endothelium. Ephrin-B2-LacZ heterozygotes stained with X-Gal are shown at E14.5. Relevant valvular expression (arrows) is demonstrated in the endothelial layer of the pulmonary valve **(A)** and tricuspid valve **(B)**. This protein expression matches in situ hybridization studies done at the same stage (data not shown). Wild-type E18.5 embryos were sectioned in a 4-chambered, transverse orientation, and sections were hybridized with a probe for ephrin-B2. Brightfield pictures **(C, E, G, I)** are shown for reference. **(C-F)** show aortic valve staining and **(G-J)** show pulmonary valve staining. Ephrin-B2 expression is seen in the endothelial layer along one edge of valve leaflets in both valves **(F, J**, arrows**)**.
(A-B) are shown at 20x magnification; **(E-F, I-J)** at 10x.
RV = Right Ventricle; Ao = Aorta

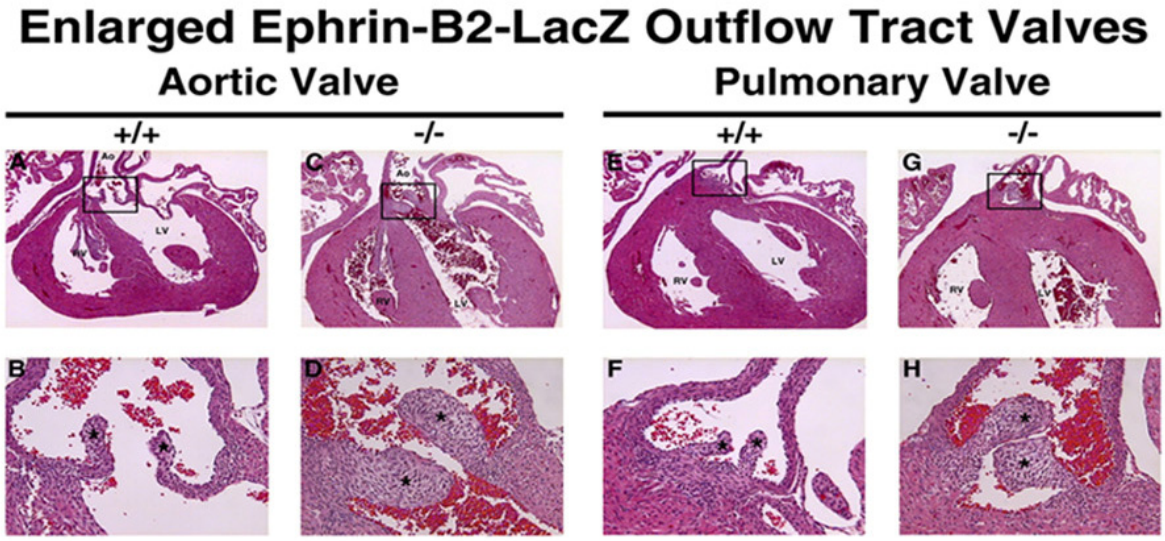

Figure 2-8. Enlarged ephrin-B2-LacZ Outflow Tract Valves. Mice sacrificed at P_0 were sectioned in a 4-chambered, transverse orientation to examine wild-type vs. homozygous targeted littermates. Aortic valve leaflets (asterisks) in the null pups **(C-D)** are enlarged in comparison to wild-type pups **(A-B)**. Pulmonary valve leaflets (asterisks) are even more grossly enlarged in comparison to wild-type littermates. Both sets of leaflets appear to have a greater number of cells as well as excess extracellular matrix. All sections are shown at 4x (top row) or 20x (bottom row). $n > 10$ for each genotype.
LV = Left Ventricle; RV = Right Ventricle; Ao = Aorta

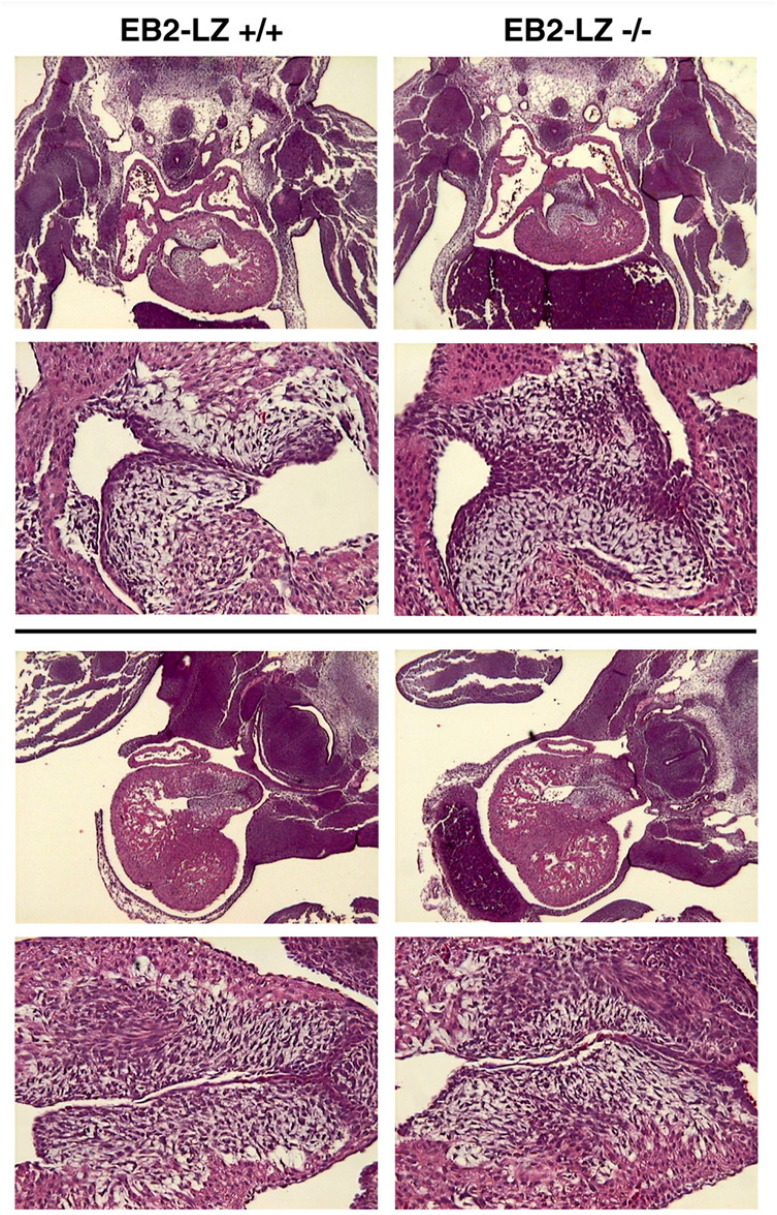

Figure 2-9. Ephrin-B2-LacZ cushion tissue is normal at E12.5. Sections of aortic **(top)** and pulmonary **(bottom)** valve cushion tissue at E12.5, as cushion formation ends and leaflet maturation begins. No difference was observed in cushion formation between wild-type littermates and ephrin-B2-LacZ homozygous-null embryos.

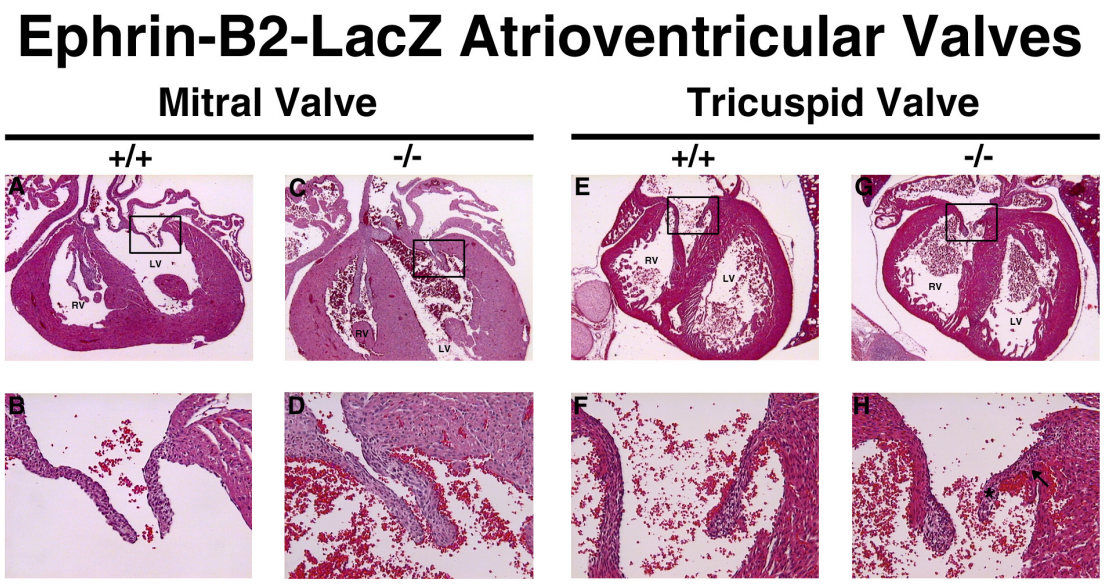

Figure 2-10. Ephrin-B2-LacZ Atrioventricular Valves. Mice sacrificed at P_0 were sectioned in a 4-chambered, transverse orientation to examine wild-type vs. homozygous targeted littermates. Wild-type **(A-B)** and homozygous null **(C-D)** mitral valves appear almost identical, with slight thickening of the mitral leaflets. The tricuspid valve in the null pups **(G-H)** shows failure of the leaflet adjoining the ventricular septum (asterisk) to properly separate from the septum (arrow) in comparison to wild-type pups **(E-F)**. All sections are shown at 4x (top row) or 20x (bottom row). n > 10 for each genotype.
LV = Left Ventricle; RV = Right Ventricle

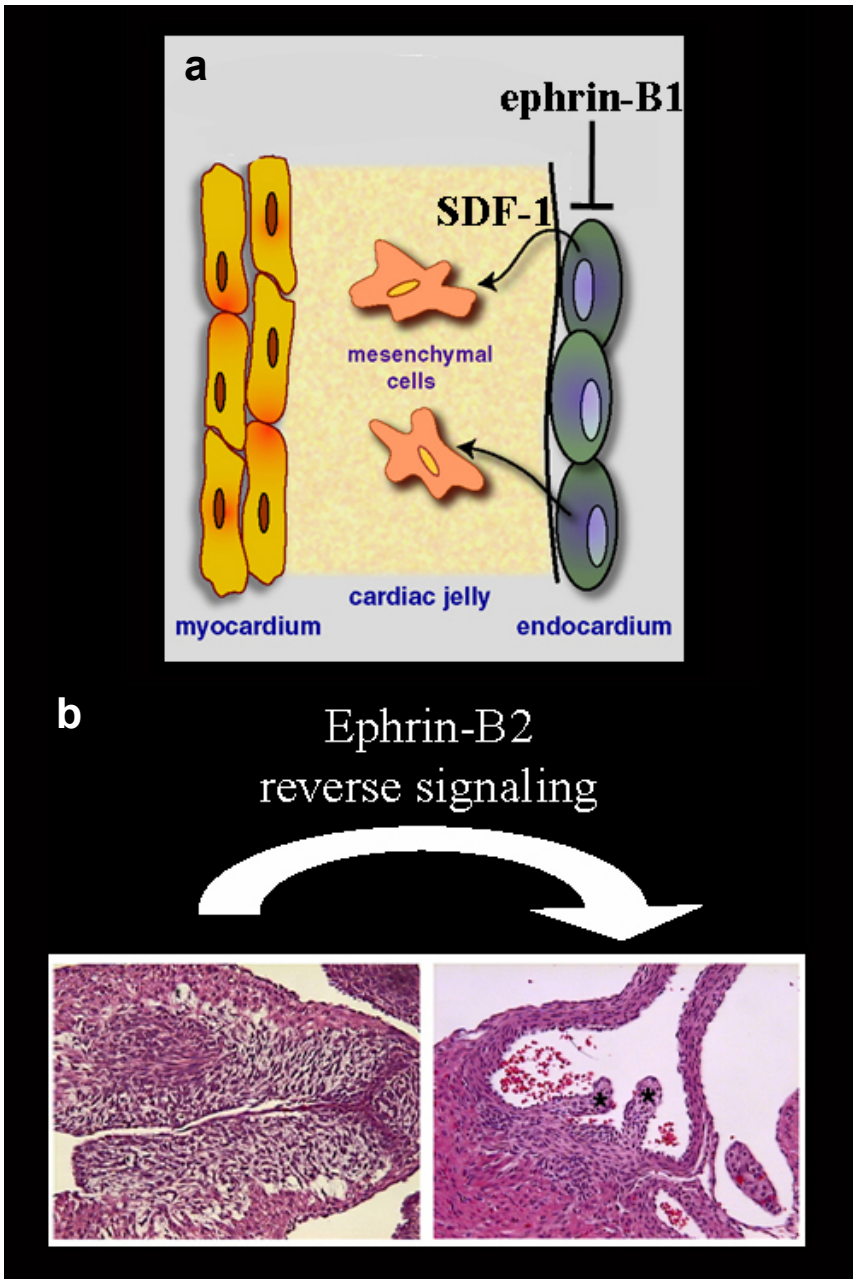

Figure 2-11. SDF-1, ephrin-B1, and ephrin-B2 in valvulogenesis. Data suggest a role for SDF-1 in attracting endothelial cells during EMT while ephrin-B1 appears to repel these cells **(a)**. Furthermore, ephrin-B2 reverse signaling appears necessary for valve leaflet maturation **(b)**.

CHAPTER THREE

THYMOSIN β4 PARTIALLY RESCUES MYOCARDIAL DAMAGE POST-INFARCTION

Introduction

Heart disease is a leading cause of mortality throughout the world. Current methods of treatment following a myocardial infarction, or a heart attack, rely predominantly on stabilizing the patient and allowing gradual partial healing to take place in the heart. However, damage sustained due to ischemia, or the deprivation of oxygen-rich blood, remains severe as collagen-based scar tissue replaces once healthy myocardium. This new tissue is not functional and thus the cardiac capacity for work is diminished.

For the purposes of this dissertation, the cardiac tissue post-infarction can be broadly divided into three different zones. The first is that in the direct area of ischemia which sustains largely irreversible cell death and scar tissue formation. This area can vary in size depending on the severity of the infarction, in effect on how much tissue is deprived completely of oxygen. Second, the area directly around the infarct zone can be thought of as bordering myocardium. Extensive literature has postulated as to the cellular changes that may occur in this area to promote cell survival and the term "hibernating myocardium" has been coined to describe tissue that, while ischemic to some degree, may eventually recover as angiogenesis and redirection of existing blood flow restores some nutrients to the area (reviewed in Bhatia et al., 2005; Depre & Vatner, 2005). While this recovery of blood flow occurs, hibernating myocardium is thought to slow down normal processes to conserve

energy and reduce resource consumption. The breadth of this partially ischemic zone of tissue is highly variable and difficult to precisely define. Finally, there remains the rest of the myocardium which may remain fully oxygenated and free of damage. One crucial change that can occur due to severe infarctions is the slow spread of cell death as partially ischemic regions of the heart do not receive blood flow restoration quickly enough to recover.

A variety of therapeutic techniques researched recently that aim to reduce cardiac damage rely on the administration of stem cells or myoblasts into the heart, a risky process. Some clinical studies that pushed ahead quickly with such therapy have encountered problems with arrhythmias and restenosis (Menasche et al., 2003; Kang et al., 2004). One potential alternative to the stem cell approach is the administration of proteins rather than whole cells to a damaged heart. Advantages of such a technique include getting around the issue of immunoreactivity that results from the introduction of allogenic cells, no need for cell culturing and preparation, greater consistency in dosage, and potentially greater diffusion of small molecules relative to that of cells.

Thymosin β4, a 43 amino acid peptide known to play both cell autonomous and non-cell autonomous roles in a variety of processes, was a candidate for this type of therapy. Thymosin β4's most well-known functions are to sequester monomeric G actin, helping to maintain a sufficient pool for cells to use in efficient synthesis of F actin polymers for use in migration, and to effect cytoskeletal organization (Safer et al., 1991; Yu et al., 1993; Sun et al., 1996; Huff et al., 2001). In addition, it is known to stimulate wound healing and angiogenesis (Malinda et al., 1999; Grant et al., 1999; Sosne et al., 2002). Thymosin β4 is widely expressed in both developing and adult mice, and work in our lab by Dr. Ildiko Bock-

Marquette has demonstrated specific expression during cardiogenesis of both RNA and protein in several cardiac muscle subtypes (Fig. 1). In addition, Dr. Bock-Marquette confirmed previous reports (Frohm et al., 1996; Grant et al., 1999; Huang et al., 2001) that thymosin β4 is secreted from cells, and she illustrated the novel concepts that thymosin β4 stimulates both endocardial and myocardial cell migration in vitro and that cultured myocardial cell survival is promoted by thymosin β4 (Fig. 2). Finally, Dr. Bock-Marquette showed that thymosin β4, the LIM domain-containing protein PINCH, and integrin linked kinase (ILK) may all bind to each other in a complex that can activate the cell survival-promoting kinase Akt (Fig. 3).

Results

Given thymosin β4's ability in vitro to increase cardiomyocyte survival and beating frequency, its activation of Akt in cultured cells, and published work from Mangi, et al. (2003) showing the beneficial effects of Akt administration post-myocardial infarction, it was reasonable to hypothesize that thymosin β4 may prove useful in repairing damage to the heart subsequent to a myocardial infarction. To test this idea, we collaborated with Dr. J. Michael DiMaio here at UT Southwestern Medical Center, in whose lab a research assistant, Mr. Michael D. White, had extensive experience creating ligations of coronary arteries in mice. With Mr. White, we created ligations of the left anterior descending coronary artery in adult male mice to cut off blood flow to a portion of the left ventricle, creating an infarct zone of injury (Fig. 4). I administered injections of PBS or thymosin β4 either near the sites of ligation, intraperitoneally, or both. Mice were then echocardiographed at various

timepoints to measure cardiac function, the measurements for which were taken by Mr. White while blinded to the experimental groups and then handed over to me for analysis. This system helped ensure that the integrity of data obtained was not influenced by investigator bias. Mice were eventually sacrificed, at which point I harvested and processed the hearts for further analysis. (see Methods section for more detail).

These studies revealed that administration of thymosin β4 dramatically improved cardiac function as assayed by echocardiography at 14 and 28 days post-ligation. Two weeks post-infarction, left ventricles of PBS-treated mice had a mean fractional shortening of 27.4 +/- 1.2% (n=23, 95% confidence interval), while thymosin β4 treatment led to a mean value of 40.5 +/- 1.2% (n=24, 95% confidence interval; $P < .0001$). At four weeks post-infarction, the mean values were 23.2 +/- 1.2% (n=22, 95% confidence interval) and 37.2 +/- 1.8% (n=23, 95% confidence intervals; $P < .0001$). As a second measure of ventricular function, two-dimensional echocardiographic measurements revealed that the mean fraction of blood ejected from the left ventricle (ejection fraction) in control mice at 2 weeks was 32.5 +/- 2.2% (n=23, 95% confidence interval), compared to a mean of 55.5 +/- 3.3% (n=24, 95% confidence interval; $P < .0001$) in thymosin β4-treated mice. At 4 weeks, the values were 28.2 +/- 2.5% (n=22, 95% confidence interval), compared to a mean of 57.7 +/- 3.2% (n=23, 95% confidence interval; $P < .0001$) in thymosin β4-treated mice (Fig. 5). The greater than 60% or 100% improvement at 4 weeks in fractional shortening or ejection fraction, respectively, suggested a significant improvement with exposure to thymosin β4, although cardiac function remained depressed compared to sham operated animals (~60% fractional shortening; ~75% ejection fraction). The degree of improvement was not statistically

different between mice given only intracardiac injections of thymosin β4, only intraperitoneal injections for systemic administration, or both. Finally, the end diastolic dimensions (EDD) and end systolic dimensions (ESD) were both significantly higher in the control group, indicating that thymosin β4 treatment resulted in decreased cardiac dilation after infarction, consistent with improved function (Fig. 5).

Based on these data, further experimentation to determine the timeframe of functional improvement showed that fractional shortening three days after infarction was 39.2 +/- 2.3% (n=5, 95% confidence interval) with intracardiac thymosin β4 treatment compared to 28.8 +/- 2.3% (n=4, 95% confidence interval) in controls ($P < .02$); ejection fraction was 64.2 +/- 6.7% or 44.7 +/- 8.4%, respectively ($P < .02$) (Fig. 6).

Histological analysis revealed a marked reduction in the size of the scar tissue area and therefore a greater amount of functional anterior wall muscle tissue in hearts treated with thymosin β4. Total protein lysate from hearts I harvested from thymosin β4-treated mice were assayed by Dr. Bock-Marquette for levels of various proteins. Concurrent with in vitro data, these experiments revealed upregulated levels of activated Akt kinase and ILK, known to activate Akt. By comparison, levels of total Akt protein did not increase. GAPDH was used as an internal control in these experiments (Fig. 7).

Immunohistochemical analysis that I did revealed a significantly decreased number of apoptotic cells at 24 hours post-ligation in the thymosin β4-treated hearts in comparison to controls (Fig. 7). This discovery correlates well with the observed increase in levels of activated Akt, as Akt has been well-described as stimulating cell survival pathways. (Please

note that experiments detailed up to this point have been published (Bock-Marquette & Saxena et al., 2004).)

Finally, experiments I did with antibodies against PECAM, Factor VIII, and isolectin B4 to stain for endocardial cells suggested that thymosin β4 administration increased angiogenesis by 72 hours post-ligation near the site of myocardial infarction. Quantitation of the isolectin B4 staining, which had the lowest levels of background noise of the three antibodies tested, revealed an approximately 79% increase in microvasculature over controls (Fig. 8). It is difficult to establish, however, if the increased amount of vasculature bordering the area of infarction is itself a direct cause of the improved cardiac function, the direct effect of thymosin β4 administration, the indirect effect of greater initial cell survival leading to recruitment of new vasculature, or a combination thereof.

Discussion

Taken together, these data suggest a potentially clinically relevant role for thymosin β4 in promoting myocardial survival and/or recovery post-ligation. Further experiments have been initiated by our lab in collaboration with the DiMaio lab to induce ligations and inject thymosin β4 in pigs. If these experiments prove successful in swine, which have hearts very similar to those in humans, the stage will then be set for eventual clinical trials in humans.

With regard to such a trial, the ability of intraperitoneal injections of thymosin β4 to be sufficient for recovery, shown here to be the case at least in mice, becomes very important. One can easily imagine the practical difficulties and perils of attempting intracardiac injections into humans. To take this supposition a bit further, then,

intraperitoneal injections, given immediately from the time of infarction in experiments described above, would be practical to give only when a human patient arrives at a care facility. As this may be some minutes or hours removed form the time of infarction, the question of how late thymosin β4 can be administered becomes an important one.

Some preliminary data from a pilot experiment attempts to address this question in mice. While 'n' values are very low, I feel the data are still striking enough in the amplitude of change to share in this discussion section as a harbinger of interesting experiments still to come. Four mice survived this experiment; one mouse given PBS starting 5 hours post-ligation, two mice given thymosin β4 starting 5 hours post-ligation, and one mouse given thymosin β4 starting 24 hours post-ligation (all injections were intraperitoneal). The 24 hours timepoint was chosen because of the previously mentioned decreased apoptosis at 24 hours post-ligation, which would imply the necessity of thymosin β4 by that point to achieve the degree of recovery observed. Mice were echocardiographed and sacrificed at two weeks post-ligation. Measuring both fractional shortening and ejection fraction as done previously, I found that thymosin β4 injection from 5 hours onward was sufficient in both mice to preserve cardiac function at levels that were seen with immediate thymosin β4 administration. Meanwhile, the one mouse receiving thymosin β4 from 24 hours onward showed values close to those of the control mouse. Clearly, the lone '24 hours' mouse here may have been a fluke in its lack of improvement, but these data are certainly intriguing enough to warrant larger scale experiments to determine up until what point thymosin β4 treatment retains its effectiveness. It is promising that in mice, thymosin β4 administration

given within 5 hours after an infarction may be sufficient for therapeutic purposes (data not shown).

Only time will tell if the potential for cardiac recovery exhibited here in mice will translate into bedside therapy. In the meantime, further preclinical experiments will be valuable in exploring both the beneficial effects of thymosin β4 administration and elucidating in more detail the downstream mechanisms and upstream regulators of this small yet efficacious protein.

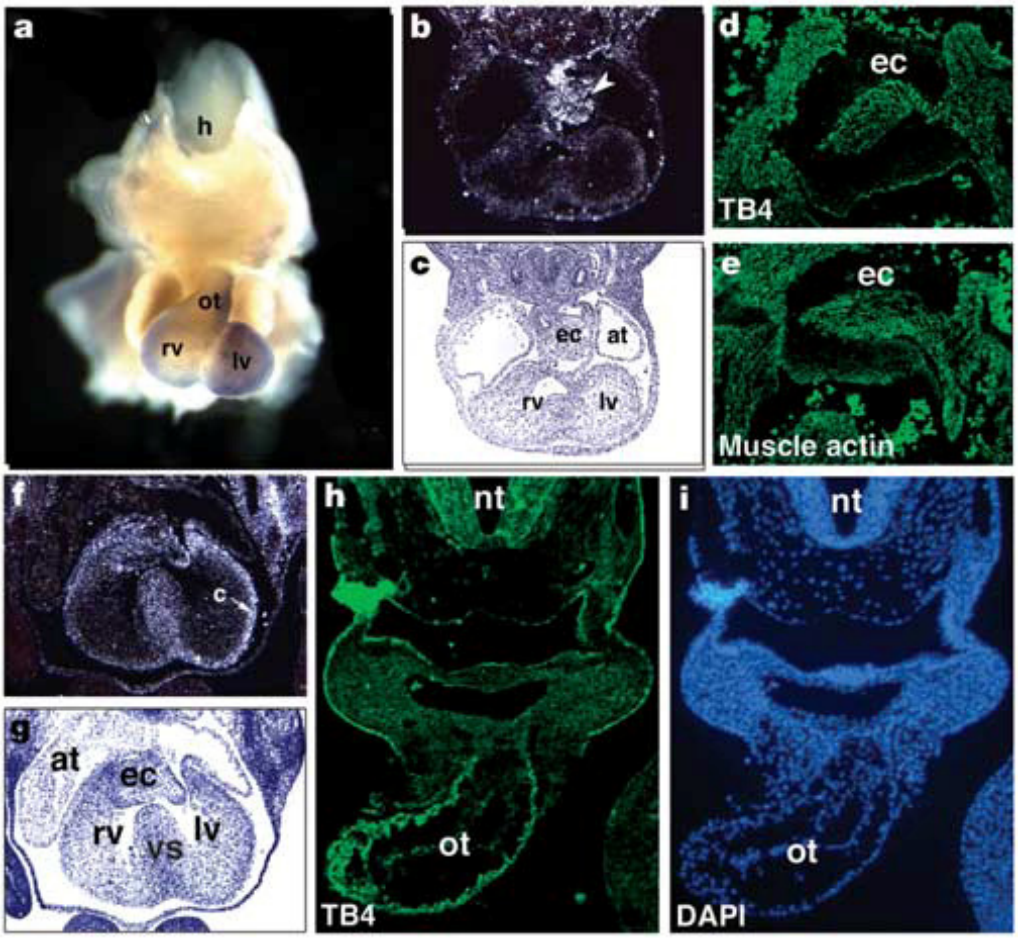

Figure 3-1. Thymosin β4 is expressed in specific cardiac cell types during development. **(a)** Thymosin β4 mRNA transcripts at E10.5 by whole-mount in situ hybridization in frontal view. **(b,c)** Radioactive section in situ hybridization at E10.5 in transverse section through heart. Arrowhead indicates endocardial cushion (ec). (**d,e**) Immunohistochemistry using TB4 **(d)** and muscle actin **(e)** antibodies focused on cushion cells at E11.5. (**f,g**) Expression of TB4 mRNA at E11.5 in compact layer (c) of ventricles and ventricular septum (vs). Note absence in atria (at). **(h,i)**, TB4 protein or DAPI in outflow tract (ot) myocardium by immunohistochemistry of E9.5 transverse section. lv, left ventricle; rv, right ventricle; h, head; nt, neural tube. (Work done by Ildiko Bock-Marquette)

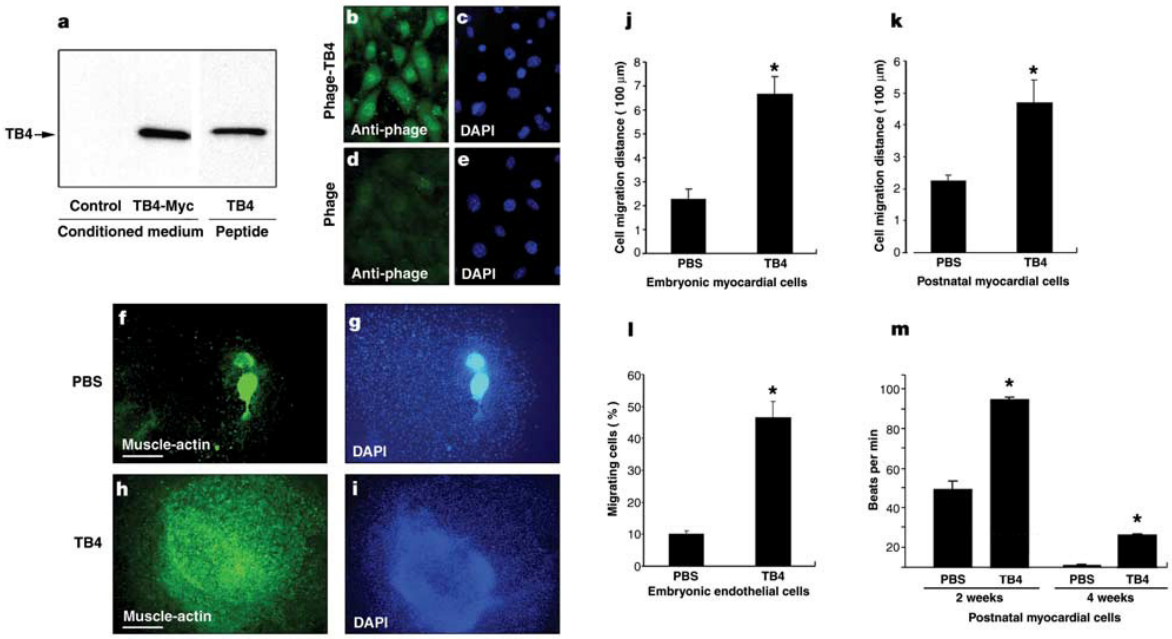

Figure 3-2. Thymosin β4 is secreted and promotes cardiac cell migration and survival. **(a)**, Western blot of supernatant from thymosin β4 (TB4) transfected Cos cells using TB4 antibodies. **(b-e)** Immunocytochemistry using anti-phage antibody or DAPI after TB4-expressing T7 phage **(b,c)** or control phage **(d,e)** administration in the medium of embryonic cardiac explants. **(f-i)** Mouse E11.5 cardiac outflow tract explants stained with anti-muscle actin antibody (green) or DAPI (blue) after PBS **(f,g)** or TB4 **(h,i)** treatment. Bars represent 500μm. Distance of migrating myocardial cells in E11.5 outflow tract explants **(j**, $P < .0001$**)** or rat neonatal cardiomyocytes **(k**, $P < .03$**)** with or without TB4 treatment. **(l)** Percent of embryonic endothelial cells migrating with or without TB4 ($P < .01$). **(m)** Beating frequency of rat neonatal cardiomyocytes with or without TB4 ($P < .05$). Means and standard deviation with 95% confidence limits are shown. *$P < .05$. (Work done by Ildiko Bock-Marquette)

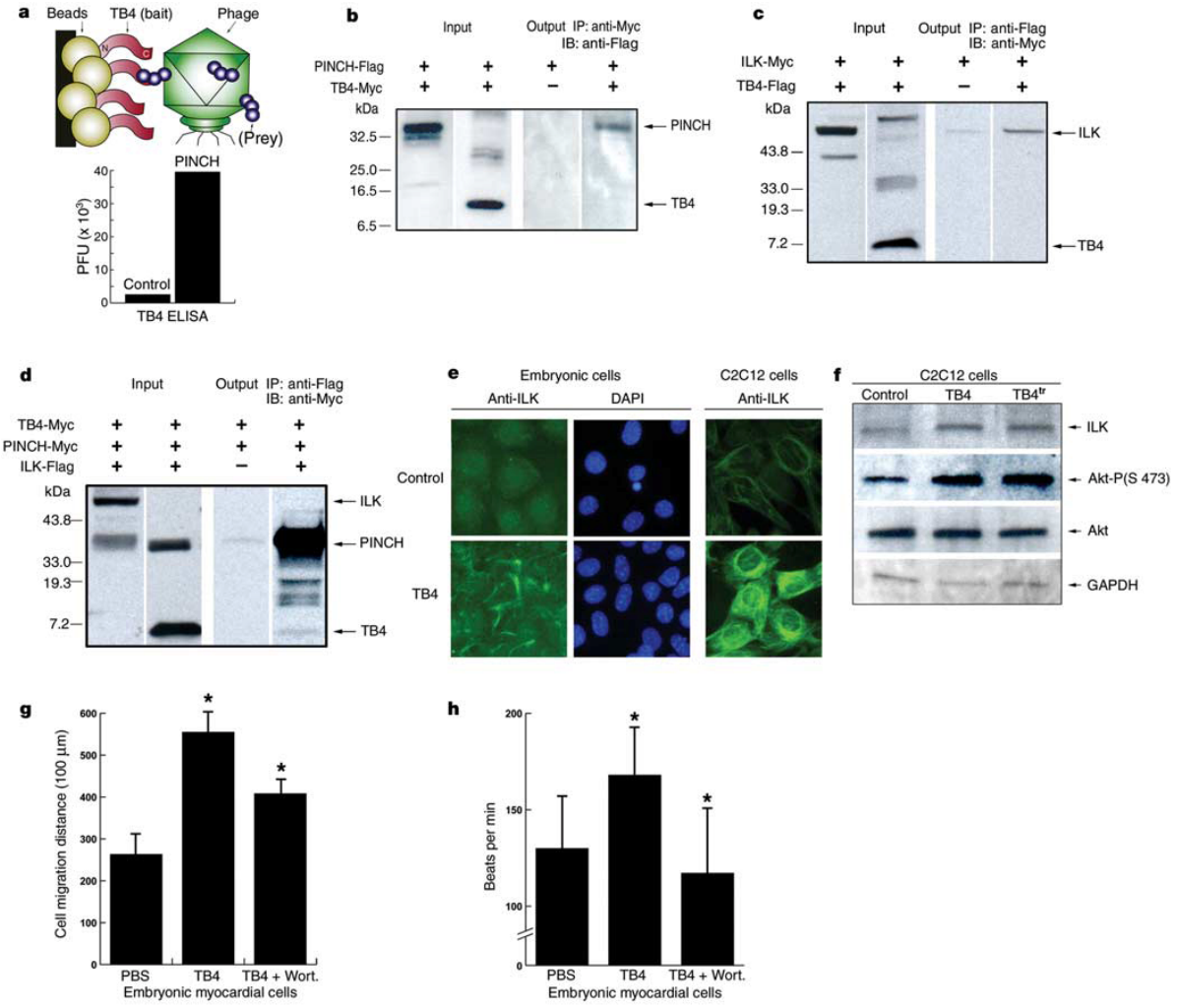

Figure 3-3. Thymosin β4 forms a functional complex with PINCH and Integrin Linked Kinase (ILK) resulting in phosphorylation of Akt. (**a**) Phage display strategy for isolating thymosin β4 (TB4) interacting proteins and ELISA confirmation of PINCH interaction. (**b,c**) Immunoprecipitation (IP) for TB4 and immunoblot (IB) for PINCH (**b**) or ILK (**c**). (**d**) IP of ILK and IB for PINCH and TB4. Cell lysate input for each protein is shown along with protein from the IP (output). (**e**) Immunocytochemistry with α-ILK antibody (green) and DAPI (blue) after TB4 treatment of embryonic cardiac explants or C2C12 myoblasts. **(f)** Western blot of C2C12 cells treated with TB4 protein or transfected with TB4-expressing plasmid ($TB4^{tr}$) using antibodies for ILK, Akt, GAPDH or phospho-specific antibody to Akt-S^{473}. **(g)** Myocardial migration or **(h)** beating frequency of E11.5 cardiac explants induced by TB4 in the presence or absence of wortmannin (Wort). Bars indicate standard deviations with 95% confidence interval. **P* < .05. (Work done by Ildiko Bock-Marquette)

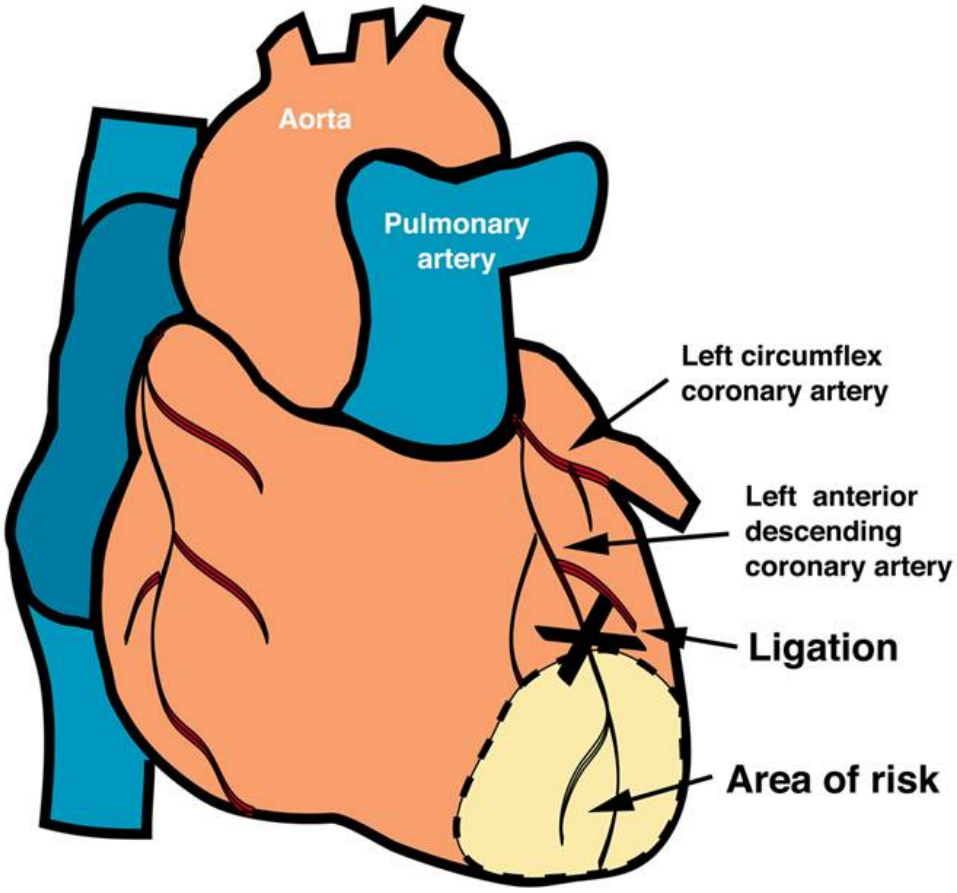

Figure 3-4. Induced Myocardial Infarction. The left anterior descending coronary artery was permanently ligated with suture, creating an area of risk where ischemia resulted in a myocardial infarction in the anterior wall of the left ventricle. Injections of thymosin β4 were then administered at either two sites next to the area of risk, intraperitoneally, or both. (Illustration courtesy of Ildiko Bock-Marquette)

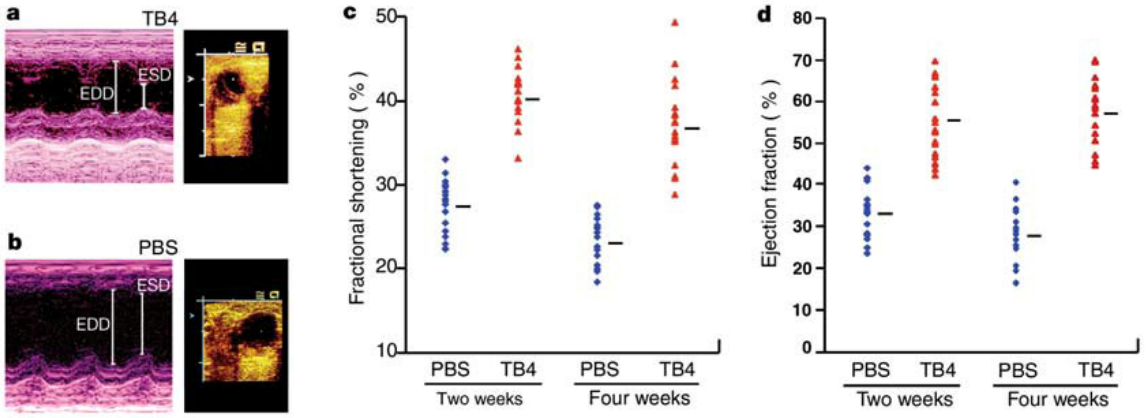

e

			EDD	ESD	FS(%)	EF(%)	Cumulative FS(%)	Cumulative EF(%)
Control ($n = 22$)	**Intraperitoneal**	**($n = 7$)**	0.567 ± 0.055	0.441 ± 0.051	22.2	33.3		
	Intraperitoneal + intracardiac	**($n = 7$)**	0.530 ± 0.049	0.412 ± 0.043	22.3	24.9	23.2 ± 1.2	28.2 ± 2.5
	Intracardiac	**($n = 8$)**	0.470 ± 0.049	0.354 ± 0.039	24.7	27.2		
Thymosin B4 ($n = 23$)	**Intraperitoneal**	**($n = 7$)**	0.502 ± 0.069	0.317 ± 0.045	36.9	54.6		
	Intraperitoneal + intracardiac	**($n = 8$)**	0.451 ± 0.063	0.296 ± 0.052	34.4	63.8	37.2 ± 1.8	57.7 ± 3.2
	Intracardiac	**($n = 8$)**	0.382 ± 0.043	0.232 ± 0.038	39.3	54.0		

* *

Figure 3-5. Thymosin β4 treatment after coronary ligation improves myocardial function in vivo. (a, b) Representative echocardiographic M-mode images of left ventricles after coronary ligation with **(a)** or without **(b)** thymosin β4 (TB4) treatment. Two-dimensional images are shown to the right. EDD, end diastolic dimension; ESD, end systolic dimension. **(c, d)** Distribution of left ventricular fractional shortening (FS) **(c)** or ejection fraction (EF) **(d)** at two and four weeks after coronary ligation with (n=23) or without (n=22) TB4 treatment. Bars indicate means. **(e)** Echocardiographic measurements for intraperitoneal, intracardiac, or intraperitoneal and intracardiac administration of thymosin β4 or PBS (Control) at four weeks. Means and 95% confidence limits are shown. **P* < .0001

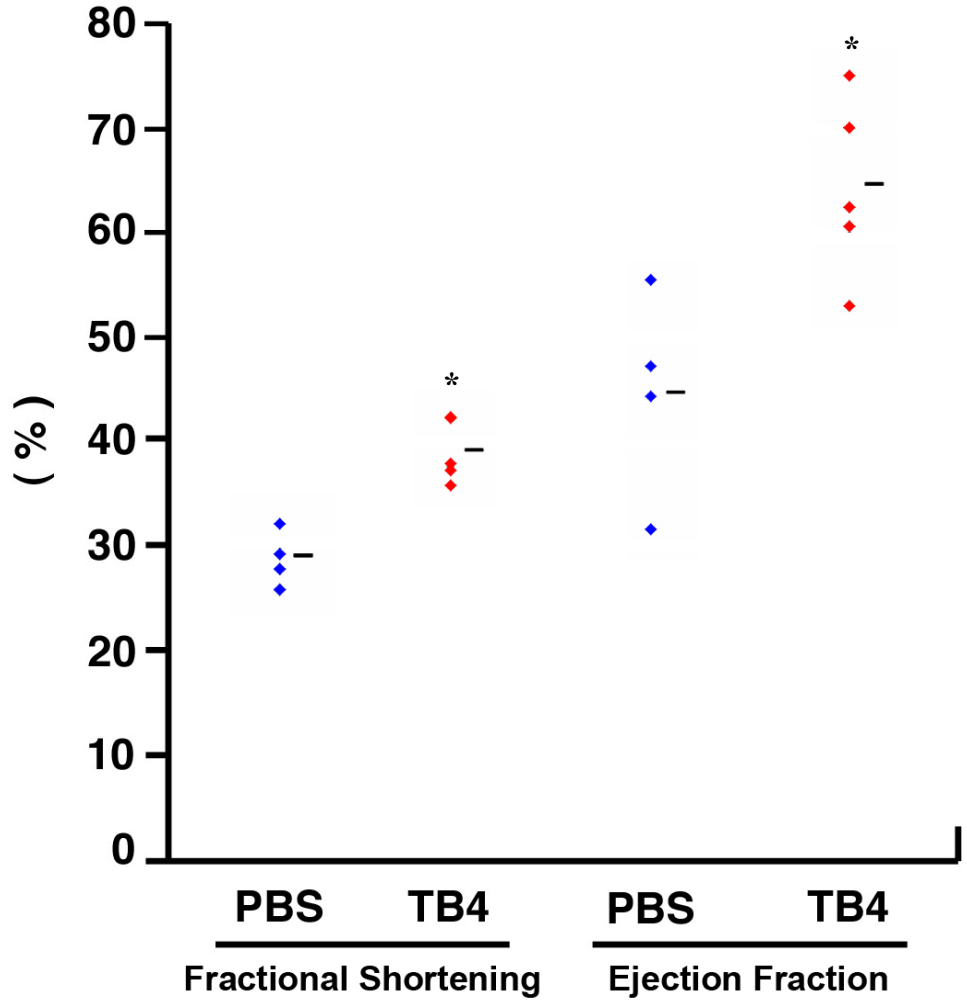

Figure 3-6. Thymosin β4 treatment improves myocardial function as early as three days post-infarction. Distribution of left ventricular fractional shortening or ejection fraction at three days after coronary ligation with (n=4) or without (n=5) TB4 treatment. Bars indicate means. *$P < .02$

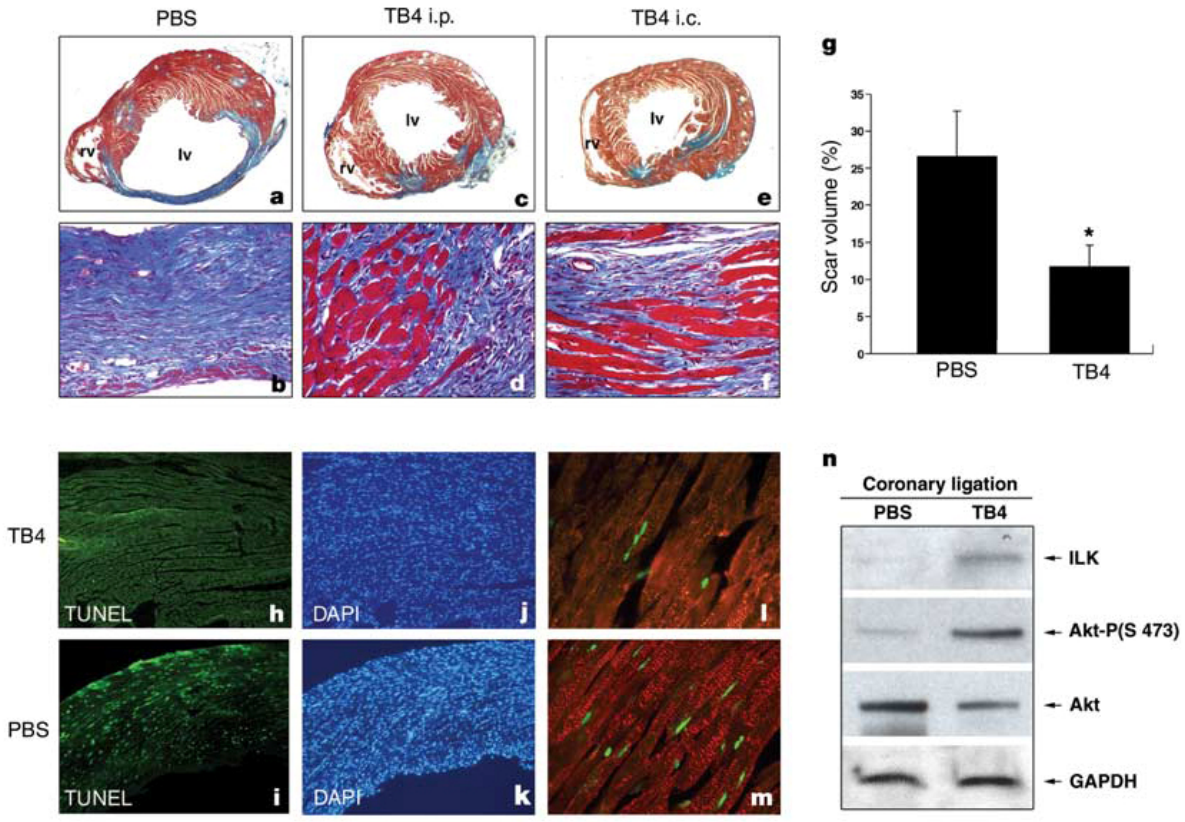

Figure 3-7. Thymosin β4 promotes survival and alters scar formation after coronary artery ligation in mice. (a-f), Representative trichrome stain of transverse heart sections at comparable levels 14 days after coronary ligation and PBS **(a,b)** or thymosin β4 (TB4) treatment delivered intraperitoneally (IP) **(c,d)** or intracardiac (IC) **(e,f)**. **(b), (d)** and **(f)** are higher magnifications of **(a), (c)** and **(e)**, respectively. Collagen in scar is indicated in blue and myocytes in red. Images are typical of twenty separate animals. **(g)** Estimated scar volume of hearts after coronary ligation and PBS or TB4 treatment. Bars indicate standard deviation at 95% confidence limits. *P < .02. **(h,i)**, TUNEL positive cells (bright green) twenty-four hours after coronary ligation and TB4 or PBS treatment. **(j,k)** DAPI stain of **(h,i)**. **(l,m)** Higher magnification of TUNEL positive nuclei (green) double-labeled with anti-muscle actin antibody (red striations) to mark cardiomyocytes. (**n**) Western blot on heart lysates after coronary ligation and treatment with PBS or TB4.

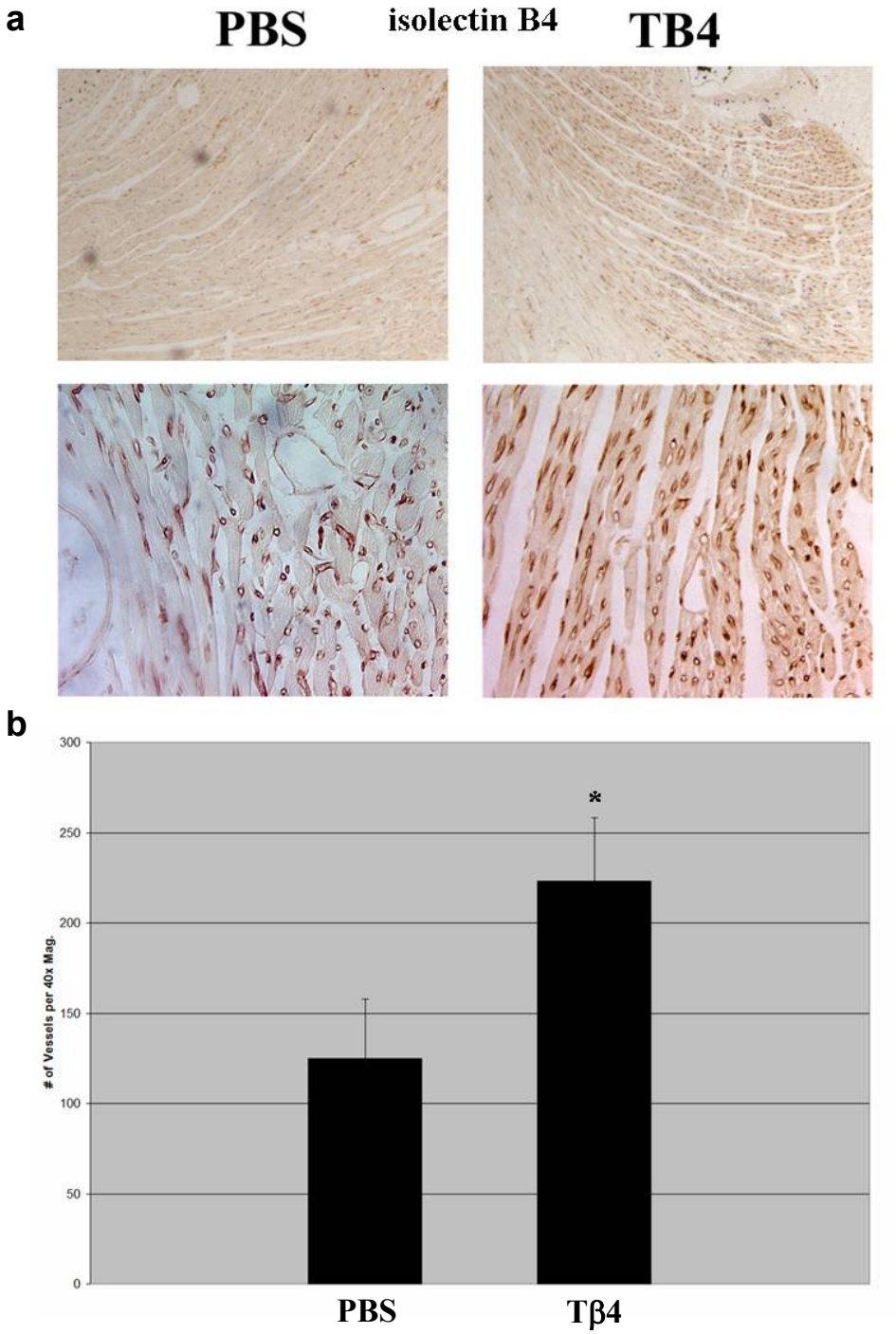

Figure 3-8. Thymosin β4 may promote angiogenesis after coronary artery ligation in mice. **(a)** Isolectin B4 staining of endothelial cells suggests a higher density of microvasculature in bordering myocardium close to the zone of injury. **(b)** Quantitated vessel density gleaned from five sections per mouse from two mice given PBS and two mice given thymosin β4. Bars indicate standard deviation at 95% confidence limits. *$P < .01$

CHAPTER FOUR

SDF-1 PARTIALLY RESCUES MYOCARDIAL DAMAGE POST-INFARCTION

Introduction

The success of the coronary artery ligation model using thymosin β4 brought me back full circle to one of the proteins I had been studying in cardiac development, SDF-1. I was interested in investigating the potential for SDF-1 to provide beneficial effects post-infarction similar to what we had seen with thymosin β4. The rationale for this line of experiments was predicated on i) published work showing the ability of SDF-1 to attract stem cells (Aiuti et al., 1997 and others) ii) evidence that, in many cell types, Akt is activated downstream of SDF-1 signaling through CXCR4 (Vlahakis et al., 2002 and others) iii) the documented ability of SDF-1 to promote angiogenesis (Mirshahi et al., 2000; Orimo et al., 2005 and others) iv) upregulated expression of SDF-1 and possibly CXCR4 as well post-infarction and in end-stage heart failure, respectively (Damas et al., 2000; Pillarisetti & Gupta, 2001) and v) some data suggesting that SDF-1 could upregulate thymosin β4 (Neuhaus et al., 2003). Cumulatively, these data suggested that SDF-1 may have a beneficial effect if injected near sites of ligation that could possibly even synergize with the thymosin β4-mediated effect.

In addition, while I was investigating this hypothesis, a number of papers were published alluding to the potential role of SDF-1 in attracting stem cells to the heart post-infarction. Specifically, reports of this stem cell attraction refer to bone marrow-derived

somatic stem cells, which fall into two main categories: hematopoietic and mesenchymal stem cells. Both types have been shown to retain the potential to differentiate into a variety of cell types both in vivo and in vitro (reviewed in Grove et al, 2004).

Work by Askari, et al. demonstrated upregulation of endogenous SDF-1 RNA post-myocardial infarction and also showed that cardiac fibroblasts expressing SDF-1 transplanted 8 weeks post-infarction attracted stem cells to the heart and improved function by 12 weeks post-infarction (2003). While interesting, this body of work looked only at late transplantation, did not investigate the physiology or mechanism of recovery, and had extremely low 'n' values for functional data.

A second publication of interest also showed upregulation of endogenous SDF-1 RNA post-infarction and went a step further to show increased levels of SDF-1 protein as well. In addition, adenoviral overexpression of SDF-1 in the heart attracted bone marrow-derived cells only if an infarction was induced first. In other words, overexpression without injury produced no attraction of bone marrow-derived cells. However, this group reported no experiments to ascertain whether or not this cell attraction improved cardiac function (Abbott, et al, 2004).

While the previous publications looked at hematopoietic stem cells, another, more recent paper looked at bone marrow mesenchymal stem cells injected within 4 days post-MI and showed that this injection improved cardiac function. SDF-1 was not part of this experiment, but this group did show that SDF-1 RNA levels post-infarction peaked early (Ma, et al, 2005).

A consensus thus seems to be forming that SDF-1 is attracting stem cells to the heart, cells that are likely improving cardiac function post-infarction. Here, I'm proposing an alternative hypothesis, namely that SDF-1-mediated improvement is at least partially due to Akt activation that is independent of stem cell recruitment. Data supporting this idea are presented in the Results section below.

Many of the published reports on stem cell differentiation into cardiomyocytes are controversial, cannot be duplicated by other groups, and/or can be explained with alternative hypotheses such as cell fusion. Putting that aside for the purposes of this dissertation, however, a survey of stem cell 'differentiation' timeframes is useful prior to detailing results in this chapter.

Beltrami, et al (2003) suggest that adult cardiac stem cells - as they hypothesize them to be – isolated, cultured in vitro, and then injected into hearts post-infarction show improved cardiac function. The earliest timepoint at which they report this is 10 days post-infarction, when they describe the new band of myocardium as thin and only partially covering the zone of injury; greater improvement is seen by 20 days post-infarction.

Hematopoietic stem cells injected are stated to cause improvement by 9 days post-infarction (Orlic et al, 2001), and a subset of hematopoietic stem cells known as side population cells injected post-infarction were not analyzed until 2 weeks post-infarction (Jackson et al, 2001).

The first of two important, simultaneous studies contradicting the idea that there is significant differentiation of stem cells into cardiomyocytes shows that three different subpopulations of labeled hematopoietic cells are present in the heart at 10 days post-

infarction but almost gone by 30 days post-infarction, do not express cardiac markers, and appear to maintain a predominantly hematopoietic fate (Balsam et al, 2004). The second study shows similar results, with the earliest analysis after infarction done at 7 days (Murry et al, 2004).

On the basis of these and other published reports, as well as common knowledge of the timeframe necessary for circulating stem cells to migrate to the heart, take up residence, and differentiate into functional cardiomyocytes, vasculature, or other useful cell types, it seems clear that any functional recovery due to stem cell administration would require several days at the very least to occur. This supposition is important to note in lieu of data presented below.

Results

Experiments I did to test the hypothesis that SDF-1 could affect myocardial function post-infarction began with intracardiac injections of SDF-1 using the same procedure as that for the thymosin β4 injections detailed in Chapter Three (also see Methods section for more detail). Echocardiography revealed that the end diastolic dimensions (EDD) and end systolic dimensions (ESD) were both significantly higher in the control group, indicating that SDF-1 treatment resulted in decreased cardiac dilation after infarction (Fig. 1 & Supplementary Movies).

At two weeks post-infarction, left ventricles of PBS-treated mice had a mean fractional shortening of 27.9 +/- 1.5% (n=9, 95% confidence interval), while SDF-1 treatment yielded a mean value of 38.1 +/- 1.5% (n=11, 95% confidence interval; $P < .0001$ vs. PBS). In addition, a small number of mice were given intracardiac injections of thymosin

β4 or both SDF-1 and thymosin β4 in the same experiment for direct comparison with SDF-1 treated mice. Two week fractional shortening values were 39.8 +/- 4.3% (n=4, 95% confidence interval) for thymosin β4-treated mice and 38.3 +/- 2.5% (n=5, 95% confidence interval) for SDF-1/thymosin β4-treated mice. Two-dimensional echocardiographic measurements revealed that the ejection fraction in control mice at 2 weeks was 35.0 +/- 7.9% (n=7, 95% confidence interval), compared to a mean of 61.9 +/- 3.7% (n=8, 95% confidence interval; $P < .0001$ vs. PBS) in SDF-1-treated mice (Fig. 2 & 3).

At four weeks post-infarction, the mean fractional shortening values were 26.8 +/- 1.2% (n=9, 95% confidence interval) for the PBS group, 39.2 +/- 2.9% (n=11, 95% confidence intervals; $P < .0001$ vs. PBS) for the SDF-1 group, 40.8 +/- 7.3% (n=4, 95% confidence intervals) for the thymosin β4 group, and 39.5 +/- 5.2% (n=4, 95% confidence intervals) for the SDF-1/thymosin β4 group. Ejection fraction values were 31.5 +/- 3.5% (n=7, 95% confidence interval) for PBS treatment and 48.8 +/- 2.4% (n=8, 95% confidence interval; $P < .0001$ vs. PBS), for SDF-1 treatment (Fig. 2 & 3). The approximately 46% or 55% improvement at 4 weeks in fractional shortening or ejection fraction, respectively, due to SDF-1 treatment was similar to the degree of improvement seen with thymosin β4 treatment. As before, cardiac function remained depressed compared to sham operated animals (~60% fractional shortening; ~75% ejection fraction).

Subsequent experiments to determine the timeframe of functional improvement showed that fractional shortening one day (24 hours) after infarction was 32.2 +/- 1.6% (n=8, 95% confidence interval) with PBS treatment compared to 40.2 +/- 1.6% (n=8, 95% confidence interval) with SDF-1 treatment ($P < .0001$); ejection fraction was 40.7 +/- 2.7%

(n=8, 95% confidence interval) or 56.6 +/- 3.7% (n=8, 95% confidence interval), respectively ($P < .0001$). (Thymosin β4 and SDF-1/thymosin β4 experimental groups were not assayed at one day.) At 3 days (72 hours) post-ligation, fractional shortening values were 30.2 +/- 1.7% (n=7, 95% confidence interval) for PBS treatment, 39.3 +/- 2.1% (n=10, 95% confidence interval) for SDF-1 treatment ($P < .0001$ vs. PBS), 39.2 +/- 2.3% (n=5, 95% confidence interval) for thymosin β4 treatment, and 35.1 +/- 2.4% (n=4, 95% confidence interval) for SDF-1/thymosin β4 treatment. Ejection fraction values were 37.0 +/- 2.9% (n=3, 95% confidence interval) for PBS treatment and 53.6 +/- 6.1% (n=5, 95% confidence interval; $P < .005$) for SDF-1 treatment (Fig. 2 & 3).

These data indicate that SDF-1-mediated functional improvement occurred as early as 24 hours post-ligation and was also observed at 3, 14, and 28 days post-ligation. Furthermore, SDF-1 treatment allowed for recovery to approximately the same levels as that seen with thymosin β4 treatment, and the combination of SDF-1 and thymosin β4 appears to have no greater effect than either one alone, suggesting a lack of synergy. One potential explanation for this observation is that the observed beneficial effects may occur through similar downstream pathways or mechanisms.

Histological analysis revealed a marked reduction in the size of the scar tissue area and therefore a thicker functional anterior wall of the heart. At 42 days post-ligation, the scar tissue percentage (of total area of tissue) as quantitated from multiple sections and animals was 10.4 +/- 2.7% in PBS-treated controls and 2.4 +/- 1.2% in SDF-1-treated animals (95% confidence interval; $P < .001$). By 63 days post-ligation, values were 22.2 +/- 5.6% and 4.6 +/- 2.8%, respectively (95% confidence interval; $P < .001$; Fig. 4).

Recently, several groups have published data alluding to the ability of SDF-1 to attract CXCR4 expressing stem cells to the heart, where they are postulated to take up residence and improve cardiac function, presumably through differentiation. In a controversial field where such differentiation is difficult to prove, however, direct evidence is lacking that these stem cells are truly becoming cardiomyocytes, vasculature, or some other beneficial cell type. Furthermore, it is unknown whether the observed rescue of function after stem cell administration is a direct or indirect effect.

While the early improvement within one day of the infarction in itself seems to rule out an initial role of stem cells, I wanted to directly ascertain any immediate stem cell presence. To this end, I looked at levels of hematopoietic stem cells present in the heart as ascertained by staining for the c-kit receptor. Significant numbers of c-kit staining cells were seen in both control and SDF-1-treated hearts at 72 hours post-infarction, and no variation was seen that correlated with PBS or SDF-1 administration (Figure 5).; even fewer stained cells were seen earlier at 24 hours post-infarction (data not shown). These negative data are important in their support for the concept of an immediate stem cell-independent effect post-infarction and are buttressed by the observed timeline of rapid improvement.

While assays for cardiomyocyte proliferation showed no change upon SDF-1 treatment (data not shown), direct evidence of decreased cell death was observed using the TUNEL assay for apoptosis. With SDF-1 treatment, the cell death caught at 24 hours post-infarction was almost completely localized to the immediate area of the infarct. Within this area as well as in the bordering myocardium, the difference in apoptosis between controls and SDF-1-treated animals was not significant (Fig. 6). However, by 72 hours post-ligation,

the apoptosis had spread outside of the immediate area of infarction to surrounding myocardial tissue in all directions in the control PBS-treated hearts. In contrast, the SDF-1-treated hearts showed little or no apoptosis outside of the area of infarct (Fig. 7). These results would suggest that bordering myocardium that is normally irreparably damaged post-infarction is rescued by SDF-1 directed cell survival.

To investigate SDF-1's potential effect on angiogenesis post-infarction, I looked at staining of PECAM and Factor VIII, known markers of endothelial cells in microvasculature. While initial results showed increased staining of both markers in SDF-1-treated infarcted hearts at 3 days post-infarction (data not shown), high background staining was also observed. A third marker, isolectin B4, which had the lowest levels of background noise of the three antibodies tested, confirmed that angiogenesis had indeed increased by 3 days post-infarction. Quantitation of the isolectin B4 staining revealed an approximately 93% increase in microvasculature over controls (Fig. 8). It is difficult to establish, however, if the increased amount of vasculature bordering the area of infarction is itself a direct cause of the improved cardiac function, the direct effect of SDF-1 administration, the indirect effect of greater initial cell survival leading to recruitment of new vasculature, or a combination thereof.

Upon investigating potential mechanisms of recovery, I found that Western blots of harvested heart cell lysates showed increased levels of ILK protein at 3 days post-infarction upon SDF-1 treatment. In addition, increased activation of Akt, a kinase downstream of ILK that is known to stimulate cell survival, was observed at both 1 and 3 days post-infarction. VEGF, a known regulator of angiogenesis, was upregulated at 1 day post-infarction; preliminary data also indicate possible upregulation at 3 days post-infarction (Fig. 9). The

VEGF upregulation correlates with the observed increase in angiogenesis by 3 days post-infarction. Finally, further preliminary data in the process of being confirmed suggest potential thymosin β4 upregulation in infarcted, SDF-1 treated hearts as well (data not shown).

These data are similar to the upregulation of ILK and activated Akt observed earlier in our published work involving administration of thymosin β4 to infarcted hearts and suggest that, similar to thymosin β4's effects, at least some of the functional rescue seen here due to SDF-1 is the result of increased Akt–mediated cell survival post-infarction. In addition, increased angiogenesis may help sustain the benefits of early cell survival over the several weeks during which cardiac function was observed to have continued improvement.

Discussion

In completing the angiogenesis experiments for this project, one point to address would be work suggesting that isolectin B4 can stain macrophages in infarcted hearts (Ismail et al., 2003) Therefore, I will stain serial sections for CD45, a marker for macrophages, to allow vascular endothelial cells to be easily distinguished both morphologically and immunohistochemically. In future experiments, it may be worthwhile to stain for vasculature in hearts well removed from the time of infarction such as those harvested at 2 weeks post-infarction as there may be lower background due to greatly decreased numbers of macrophages.

While I do not rule out a role for stem cells in improving cardiac function over time, developmental studies suggest that the observed improvement of function at both 24 and 72

hours post-infarction is too immediate to be accounted for by stem cells migrating to the heart, taking up residence, and differentiating into functional cardiomyocytes, a process that developmental dogma suggests would take days if not weeks, not 24 hours (see Introduction for more detail). Therefore, I suggest that any cardiac functional improvement may be multifactorial in its causes but that the remarkable initial conservation of function is likely to be due to preservation of myocardial tissue bordering the immediate area of infarct. This preservation may be directed through an Akt-mediated pathway and is not likely, at least initially, to be related to stem cell recruitment and differentiation. I will soon be repeating experiments to confirm the aforementioned preliminary data on thymosin β4 upregulation in SDF-1 treated hearts, which could establish a novel connection to Akt as well as explain the lack of synergy with dual SDF-1/thymosin β4 administration.

While both SDF-1 and thymosin β4 proved able to restore cardiac function, presumably through being able to diffuse easily given their small size and structure designed for signaling over distances, a third protein tested, the aldose reductase inhibitor sorbinil, did not prove efficacious in improving cardiac function. In a pilot experiment I attempted for a variety of reasons, there was no statistical difference in fractional shortening between mice treated with PBS and those treated with sorbinil (data not shown). These data are worth mentioning as a control in reference to the improvement mediated by SDF-1 and thymosin β4. In other words, not every protein tested in this coronary artery ligation model improves cardiac function, a reassuring fact for any researcher.

The last several years have seen more and more attention being paid to cardiac injury, recovery, and potential therapy, usually focused on utilizing adult stem cells of various types.

In addition, the previously accepted dogma of an adult mammalian heart incapable of cardiomyocyte cell division is also being challenged by a few researchers in the field. In the midst of these exciting developments, there exists the somewhat dangerous potential of focusing solely on adult stem cells at the expense of other approaches of therapeutic interest. The growing body of work on treatment post-infarction utilizing SDF-1's ability to attract CXCR4-expressing stem cells may be a small example of such a focus. Data that I've accumulated suggest that stem cells are not necessary to produce an SDF-1-mediated therapeutic effect, at least initially. While this most certainly does not rule out a stem cell-mediated effect later on, published work thus far has not attempted to answer this question. To the contrary, current evidence for stem cell recruitment being the actual cause of the improvement is circumstantial. No group has been able to show that stem cells recruited by SDF-1 are actually differentiating into cardiomyocytes, vasculature, or some other beneficial cell type. In addition, the functional data that are presented are not impressive in their statistical significance. Therefore, I hope to contribute something significant to the field with data suggesting statistically significant improvement of cardiac function as a result of SDF-1 administration that appears to predominantly affect myocyte survival and possibly angiogenesis at an early timepoint.

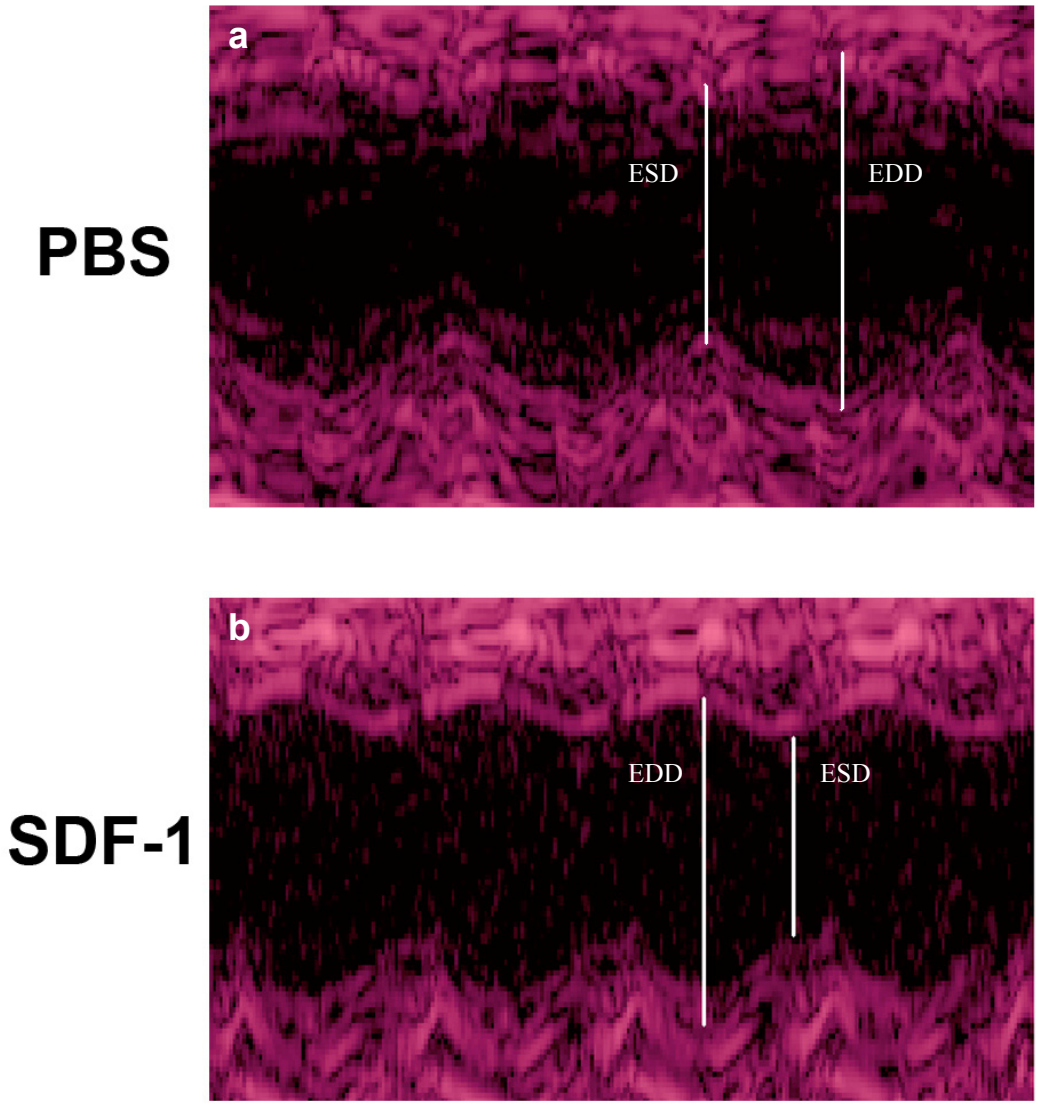

Figure 4-1. SDF-1 treatment after coronary ligation improves myocardial function in vivo. Representative echocardiographic M-mode images of left ventricles after coronary ligation with **(b)** or without **(a)** SDF-1 treatment. EDD, end diastolic dimension; ESD, end systolic dimension.

(See Supplementary Movies for 2-D echocardiography of PBS and SDF-1 treated hearts.)

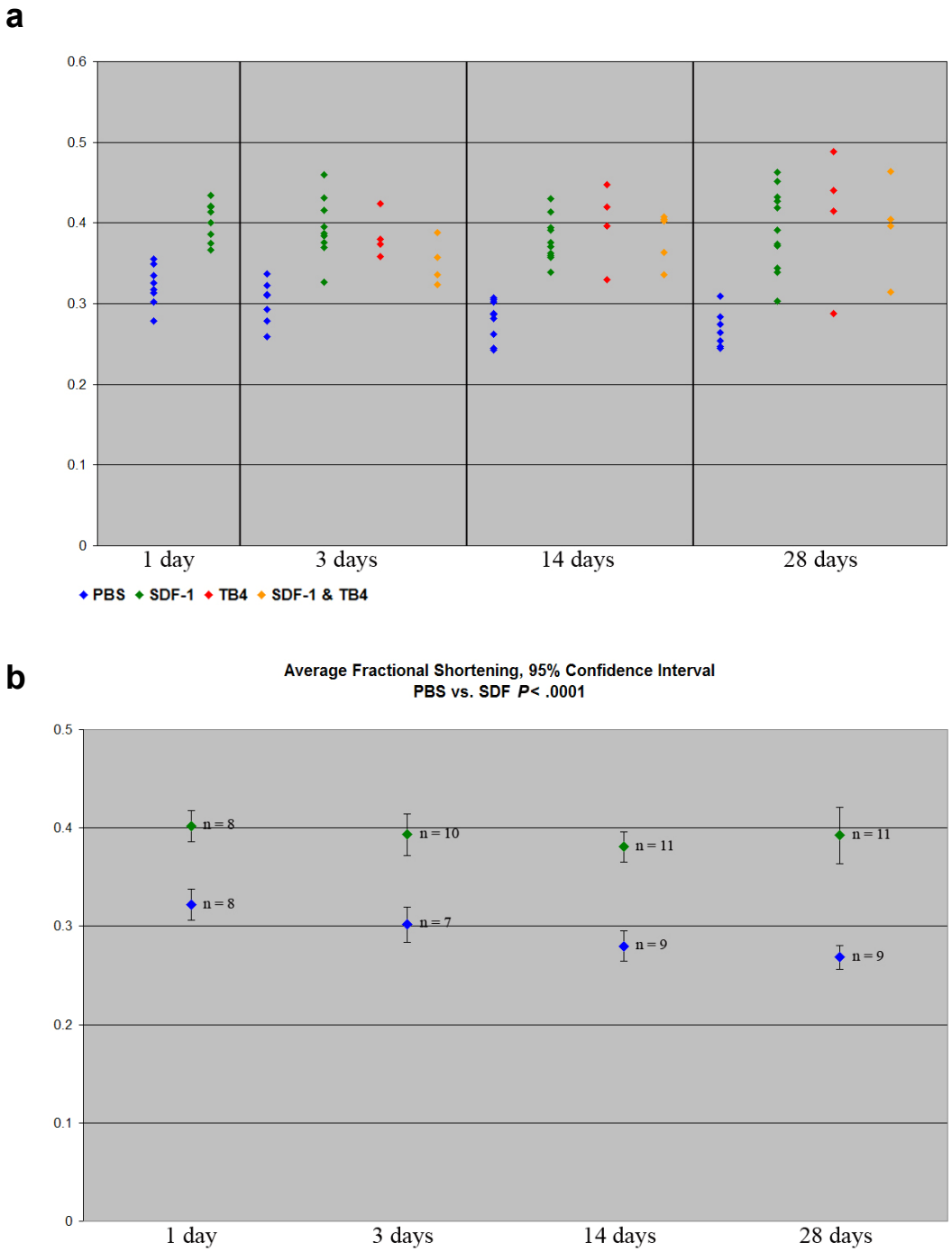

Figure 4-2. SDF-1 treatment after coronary ligation improves fractional shortening in vivo to levels comparable to those after thymosin β4 treatment. (a) Distribution of left ventricular fractional shortening at one, three, fourteen, and twenty-eight days after coronary ligation with no treatment or SDF-1 treatment. A small number of mice in the same experiment were given thymosin β4 or both SDF-1 and thymosin β4 for direct comparison. **(b)** Means, 95% confidence limits, and 'n' values are shown for PBS and SDF-1 treated animals at each timepoint. **P* < .0001

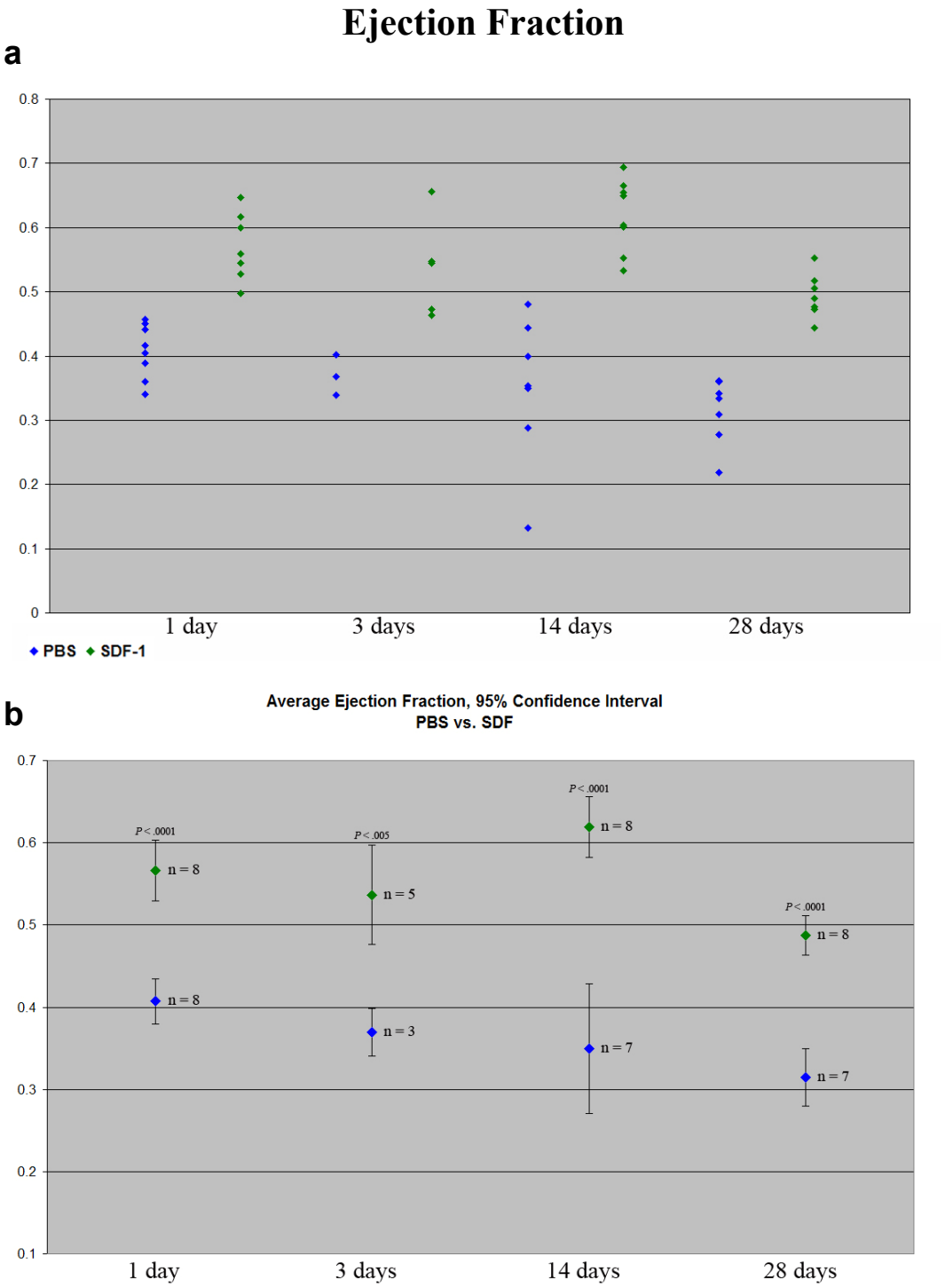

Figure 4-3. SDF-1 treatment after coronary ligation improves ejection fraction in vivo. **(a)** Distribution of left ventricular ejection fraction at one, three, fourteen, and twenty-eight days after coronary ligation with no treatment or SDF-1 treatment. **(b)** Means, 95% confidence limits, and 'n' values are shown for PBS and SDF-1 treated animals at each timepoint. *$P < .0001$ except at 3 days ($P < .005$)

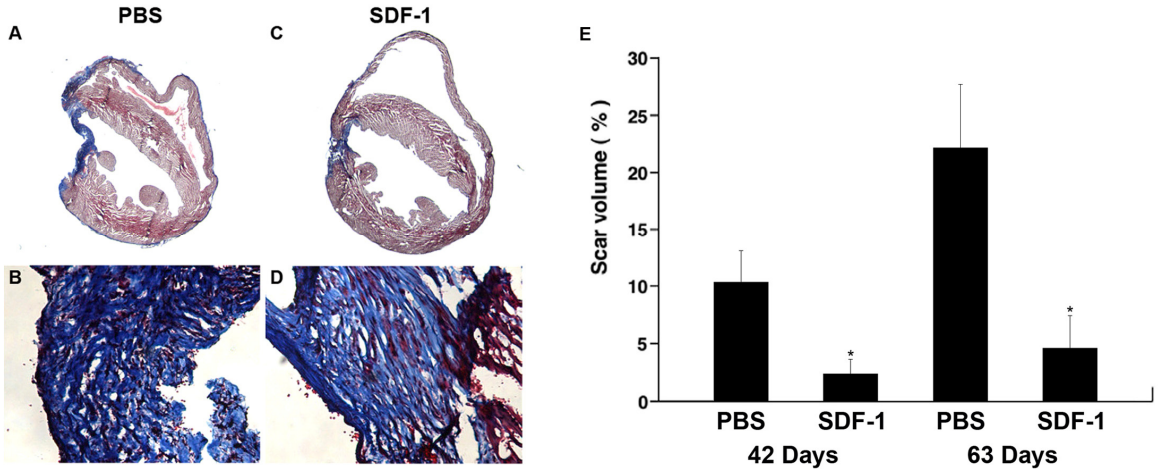

Figure 4-4. SDF-1 reduces levels of scar tissue post-infarction. **(a)** Representative trichrome stain of transverse heart sections 42 days after coronary ligation and PBS **(A,B)** or SDF-1 **(C,D)** treatment. Collagen in scar is indicated in blue. Higher magnifications illustrate the increased amount of underlying myocardium present amongst scar tissue in SDF-1-treated hearts **(D)** in comparison to PBS-treated hearts **(B)**. **(E)** Quantitated scar volume of hearts after coronary ligation taken from five sections per mouse from four mice given PBS and five mice given SDF-1. Bars indicate 95% confidence limits. **P* < .001

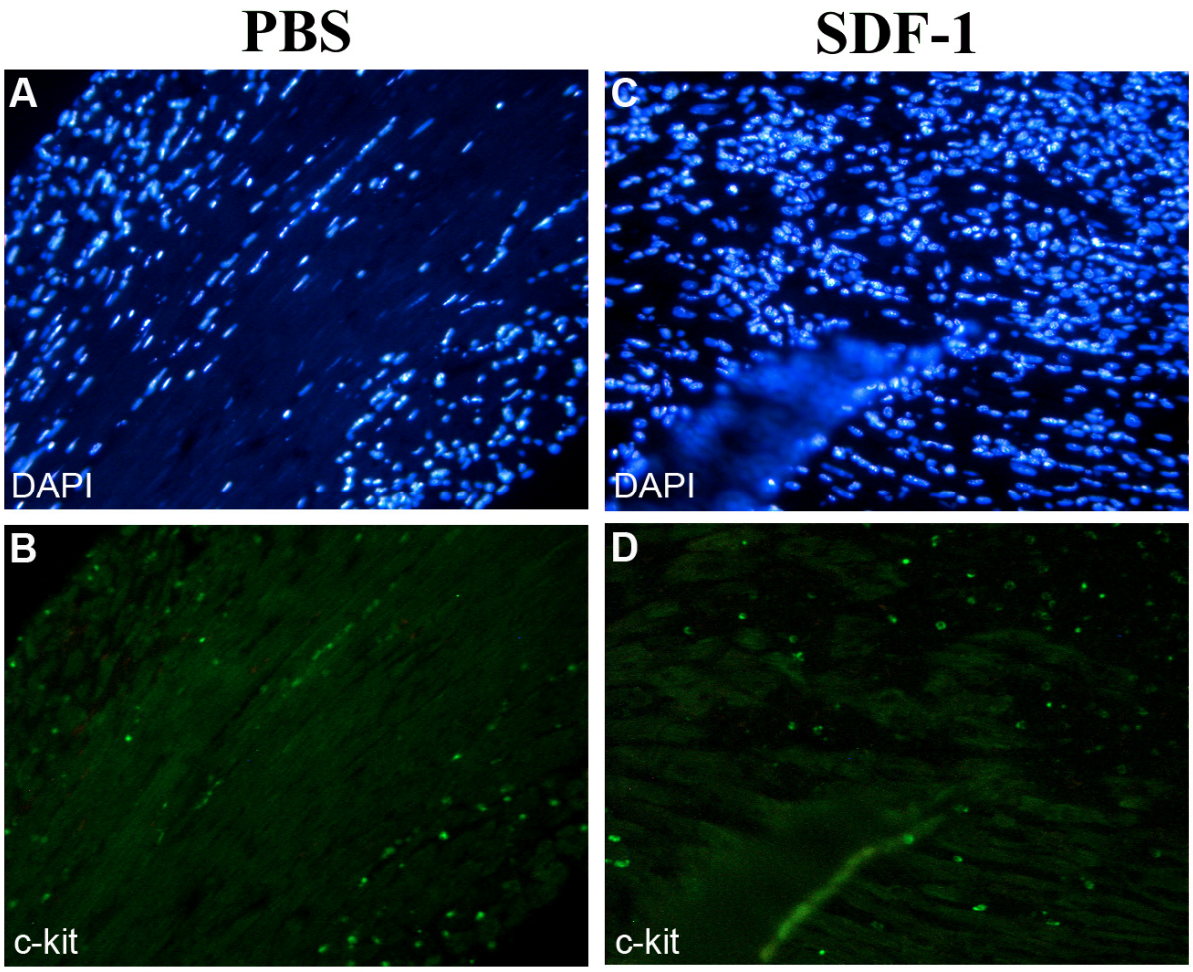

Figure 4-5. C-kit staining for hematopoietic stem cells is negative at 72 hours. No significant change was seen in the number of c-kit staining cells (bright green) at 72 hours post-infarction upon SDF-1 treatment **(D)** in comparison to PBS treatment **(B)**. Note the large band of myocardium absent of DAPI-staining nuclei (blue) in the heavily damaged PBS-treated heart **(A)** in comparison to SDF-1 treated myocardium **(C)**.

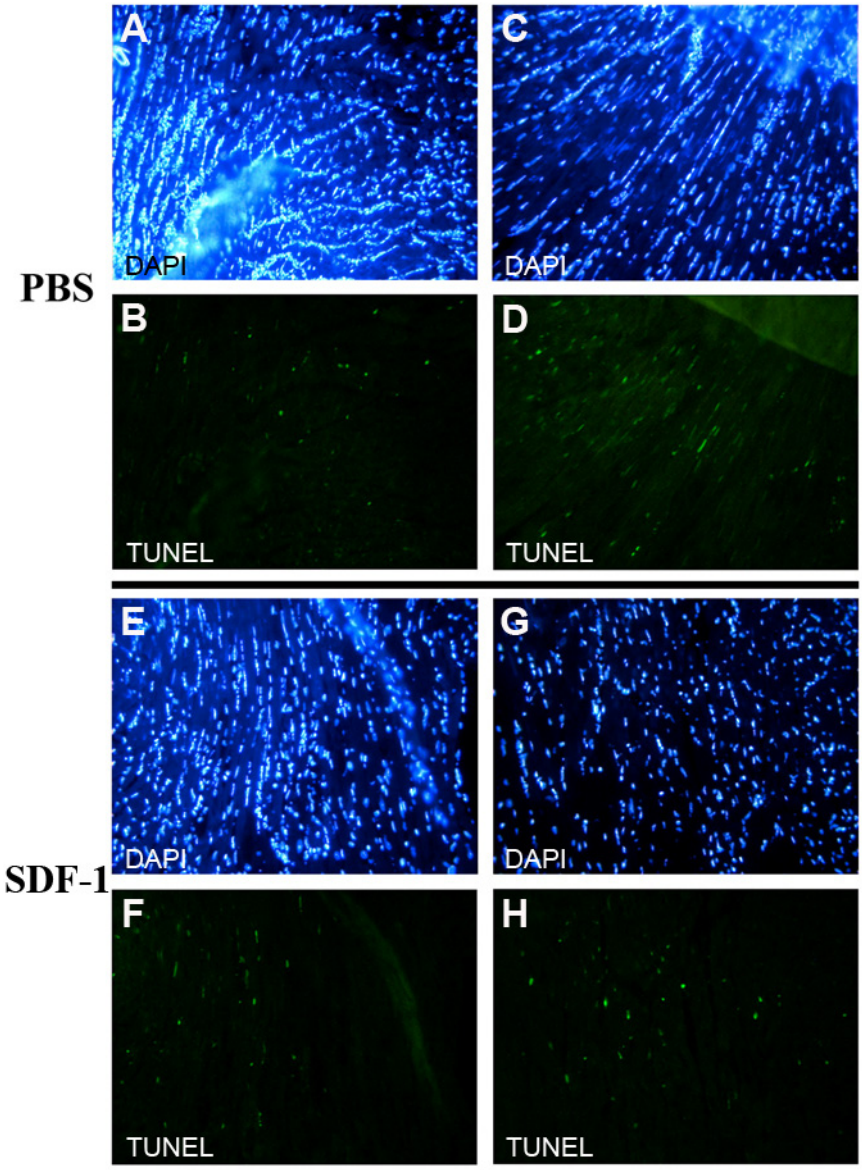

Figure 4-6. Apoptosis at 24 hours post-infarction in both the infarct area and bordering myocardium. TUNEL positive cells (bright green) twenty-four hours after coronary ligation and PBS **(B,D)** or SDF-1 **(F,H)** treatment. The left column illustrates examples of the zone of infarct, as evidenced by the distorted nuclear DAPI staining (blue) (**A,E)**. The right column illustrates bordering myocardium near the zone of infarct. No significant difference in cell death was observed at this timepoint in either of the two areas. Apoptosis is mostly confined to the infarct zone and closely surrounding tissue.

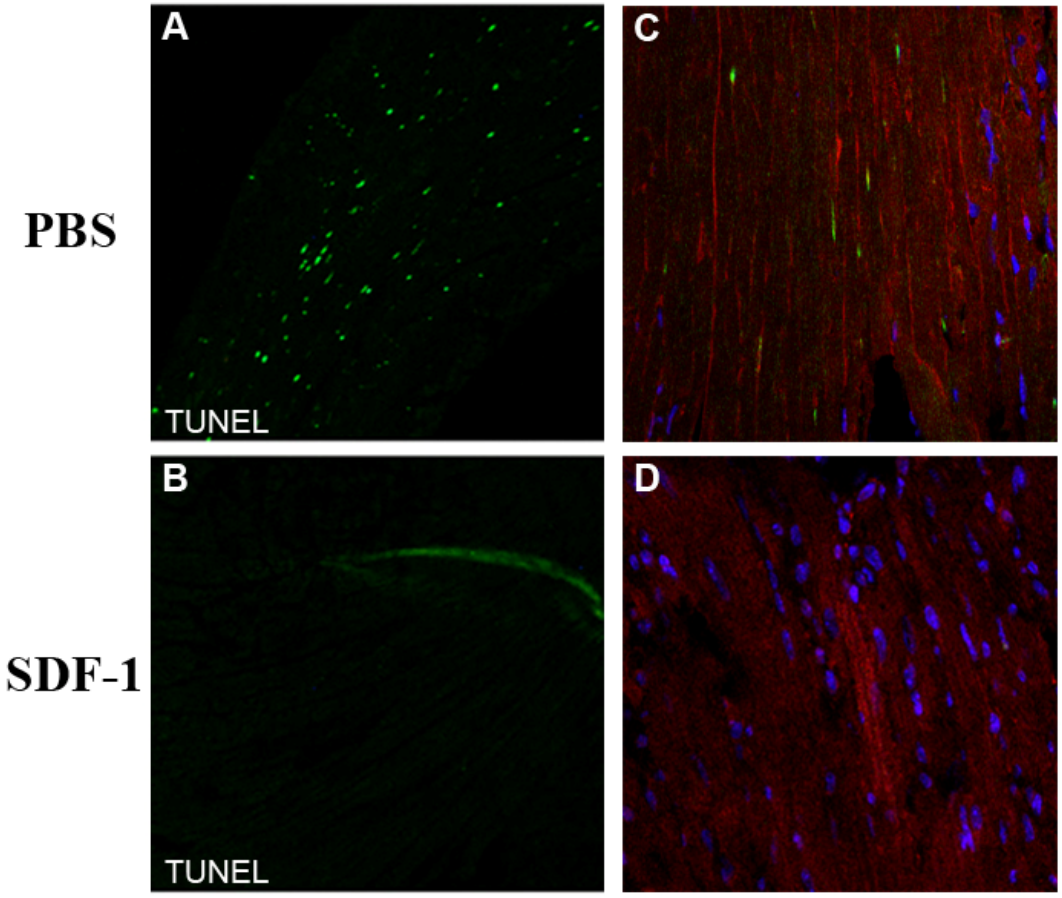

Figure 4-7. Apoptosis at 72 hours post-infarction in bordering myocardium. TUNEL positive cells (bright green) seventy-two hours after coronary ligation and PBS **(A,C)** or SDF-1 **(B,D)** treatment. The left column illustrates low-magnification views **(A,B)** of bordering myocardium. The right column illustrates higher magnification of TUNEL positive nuclei triple-labeled with anti-muscle actin antibody (red striations) to mark cardiomyocytes and DAPI (blue) to mark all nuclei. Cardiomyocytes undergoing apoptosis are prevalent after PBS treatment **(C)** but absent after SDF-1 treatment **(D)**. Note the near absence of DAPI staining in the PBS-treated damaged tissue **(C)**.

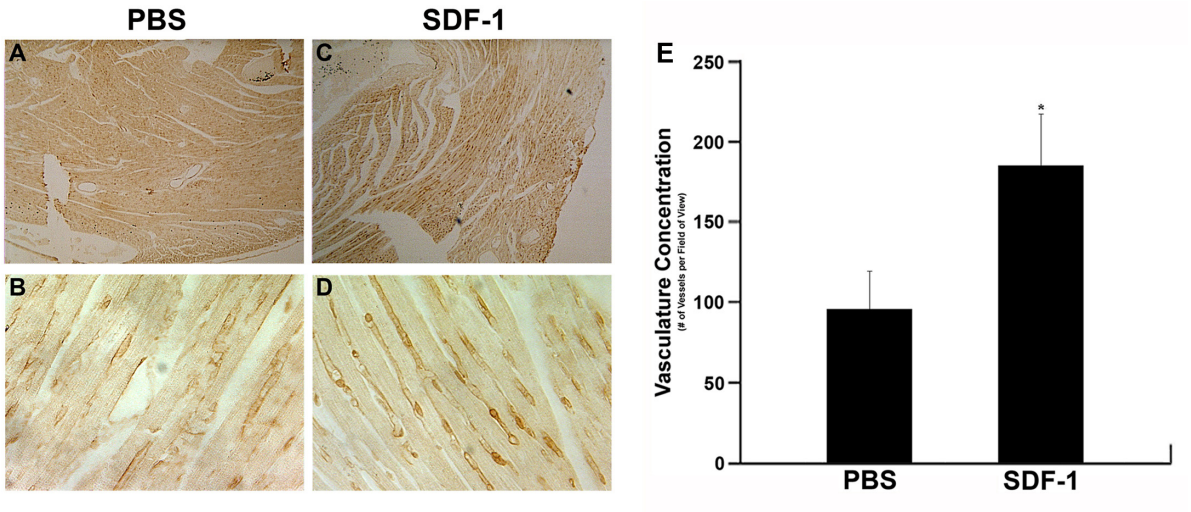

Figure 4-8. SDF-1 promotes angiogenesis after coronary artery ligation in mice. Isolectin B4 staining of endothelial cells demonstrates a higher density of microvasculature in bordering myocardium close to the zone of injury after SDF-1 treatment **(C,D)** in comparison to PBS treatment (**A,B**). **(E)** Quantitated vessel density gleaned from five sections per mouse from two mice given PBS and two mice given SDF-1. Bars indicate 95% confidence limits. **P* < .005

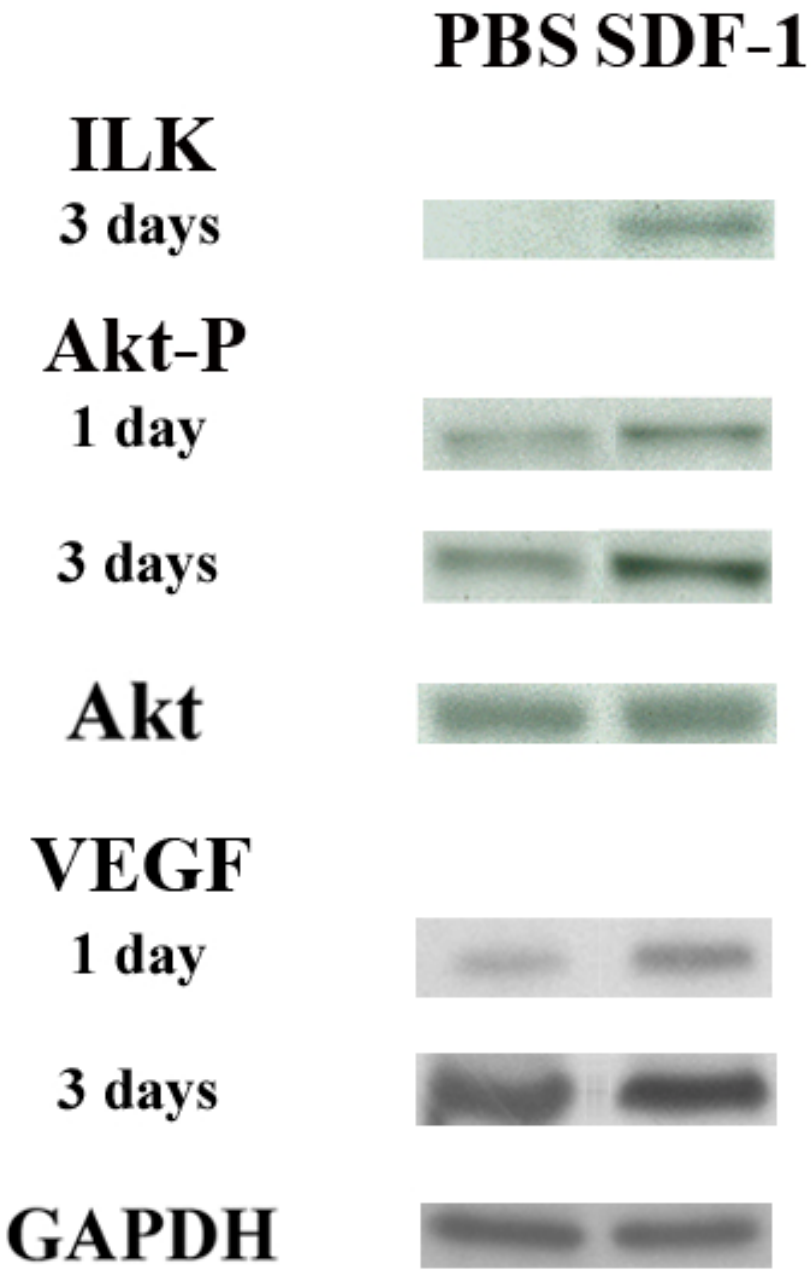

Figure 4-9. Western blots with heart lysates after coronary ligation and treatment with PBS or SDF-1. ILK at three days post-infarction and activated, phosphorylated Akt at one and three days were upregulated after SDF-1 treatment. Levels of Akt overall did not change. VEGF was upregulated at one day; preliminary data indicate an upregulation at three days as well.

METHODS

RNA in situ hybridization

Expression of SDF-1, CXCR4, ephrin-B1, and ephrin-B2, and thymosin β4 was characterized through either whole-mount or section RNA in situ hybridization of E 9.5-18.5 mouse embryos with digoxigenin-labeled or ^{35}S-labelled antisense riboprobes, respectively, as previously described (Nakagawa et al., 1999; Yamagishi et al., 2003). Sense probes were used as negative controls. Antisense probes were made from linearized plasmids containing cDNA fragments with the following primers and enzymes: SDF-1 – SpeI, T7; CXCR4 – EcoRV, T7; ephrin-B1 – NotI, T3; ephrin-B2 – NotI, T3. Thymosinβ4 antisense probe was made from the 3' UTR region of mouse thymosinβ4 cDNA that did not share homology with the closely related transcript of thymosin β10.

Collagen gel migration assay

In vivo EMT into a collagen-based extracellular matrix was imitated using an in vitro collagen gel assay widely used to study valve precursor formation (Bernanke & Markwald, 1982; Runyan & Markwald, 1983; Wunsch et al., 1994; van den Hoff et al, 1999). Cells undergoing epithelial-mesenchymal transformation (EMT) invade the collagen gel.

For experiments with SDF-1 and ephrin-B1, atrioventricular canal tissue was dissected from E10.5 or E11.5 wild-type mouse embryos and placed on collagen matrices as previously described with the endothelial surface facing down (Runyan et al., 1983). The collagen gel was prepared with (a) either no protein, 8 ug/ml BSA, 2 ug/ml ephrin-B1, 4 ug/ml ephrin-B1,

or 8 ug/ml ephrin-B1 throughout the gel or (b) with no protein throughout the gel but instead with protein-soaked beads spotted in the polymerizing gel. Explants were incubated at 37^{o}C 5% CO_2. Migration was assayed and photographed every 12 hours after placement of explants. Several experiments revealed useful timepoints to assay; Chapter One, Figure 5 illustrates migration 42 hours post-explantation, a key timepoint when explants have had time to attach, restart contraction, and migrate to a significant degree but not so late as to have explant viability deteriorate. For experiments with protein throughout the gel, migration distance was quantitated using Openlab 3.03 software (Improvision). 8 measurements of migration distance were taken per explant at angle increments of 45° while blinded to the experimental groups. For experiments with beads, explants were scored as a whole in direction of migration while blinded to the experimental groups.

For experiments with thymosinβ4, Ildiko Bock-Marquette dissected out outflow tract tissue at E11.5. After 10 hours of attachment, explants were incubated in 30ng/300µl thymosin β4 in PBS, PBS alone or thymosin β4 and 100nM wortmannin. Explants left in culture long enough will exhibit myocardial cell migration after endocardial cells have migrated. Therefore, cultures were carried out for 3-9 days. Cells were counted for quantification of migration and distance.

Preparation of beads for collagen gel migration assay

Macroprep CM Support (Bio-Rad, # 158-0070) chromatography matrix 50 um beads were used for binding BSA, SDF-1, or ephrin-B1. Beads were first washed with pre-wash buffer

and deionized water, then equilibrated with running buffer as suggested by Bio-Rad literature. Equilibration pH was tailored to the individual proteins (SDF-1 pI ~ 9.0; ephrin-B1 pI ~ 7.8). Beads were then soaked with the proteins at room temperature for 1 hours. Gels were induced to polymerize with the addition of $NaHCO_3$, and beads were immediately spotted into the polymerizing gel. Explants were added after gel polymerization as before.

Ephrin-B2-Lac Z mice analysis

Mice harboring an Ephrin-B2-LacZ targeted deletion were obtained from M. Henkemeyer's laboratory at UT Southwestern Medical Center. Genotyping was done by PCR with the following primers: EB2-1 (TCTGTCAAGTTCGCTCTGAGG); EB2-2N (CTTGTAGTAAATGTTGGCAGGACT); LZ (AGGCGATTAAGTTGGGTAACG). EB2-1 and EB2-2N yielded a wild-type 500 bp band while EB2-1 and LZ yielded a mutant 400 bp band. LacZ staining was done on whole embryos after fixation with standard protocols using X-gal (Henkemeyer et al., 1996).

Valve defects were ascertained by studying multiple serial sections per mouse, with greater than 10 animals analyzed per genotype. Wild-type and homozygous-null embryos and pups were cut in a near-transverse orientation for histological analysis of the hearts. Cell number quantitation was performed with the aid of Openlab 3.03 software (Improvision) after DAPI staining of nuclei.

Immunocytochemistry on collagen gel explants

Ildiko Bock-Marquette permeabilized paraformaldehyde-fixed explants for 10 min at RT with Permeabilize solution (10mM PIPES pH6.8; 50mMNaCl; 0.5% Triton X-100; 300mM Sucrose; 3mM $MgCl_2$) and rinsed with PBS 2 x 5 min at RT. After a series of blocking and rinsing steps, detection antibodies were used and explants rinsed and incubated with Equilibration buffer (Anti-Fade kit) 10 min at room temperature. Explants were scooped to a glass microscope slide, covered, and examined by fluorescein microscopy. TUNEL assay was performed using ApopTag Plus Fluorescein In Situ Apoptosis detection kit (Intergen Company # S7111).

Coimmunoprecipitation

Ildiko Bock-Marquette transfected Cos and 10T1/2 cells with thymosin β4, PINCH and/or ILK and lysates precipitated with antibodies to each. Western blots were performed using anti-ILK polyclonal antibody (Santa Cruz), anti-thymosin β4 polyclonal antibody (gift of H. Yin) and anti-myc or anti-FLAG antibody against tagged versions of PINCH.

Animals and surgical procedures

Myocardial infarction was produced in male C57BL/6J mice at 16 weeks of age (25-30 g) by ligation of the left anterior descending coronary artery with 8-0 prolene suture similar to that previously described (Garner et al., 2003). For initial experiments with thymosin β4 assayed at 14 and 28 days post-infarction, 45 mice survived the ligations and were echocardiographed. (22 had received PBS and 23 had received thymosin β4 through either

intracardiac injections, intraperitoneal injection, or both). Initial experiments with SDF-1 assayed at 14 and 28 days post-infarction had 20 surviving mice (9 had received PBS and 11 had received SDF-1, all through intracardiac injections). In addition, 4 mice received both thymosin β4 and SDF-1 through intracardiac injections. Additional mice were operated on in a similar fashion and echocardiographed to assay function and/or sacrificed for various experimental analyses at 0.5, 1, 3, 42, and 63 days after ligation (see Chapter Three, Figures 5 & 6; Chapter Four, Figures 2 - 4).

Two intracardiac injections per heart were administered into myocardium adjacent to the ischemic zone at the time of ligation. Each injection was 5 ul of one the following in a collagen base: PBS; synthetic thymosin β4 (RegeneRx Biopharmaceuticals, Inc.) at a concentration of 40 ng/ul; recombinant (amino acids 22 – 89) mature mouse SDF-1α protein (R & D Systems, catalog # 460-SD-010) at a concentration of 60 ng/ul; both thymosin β4 and SDF-1 α at 40 ng/ul and 60 ng/ul, respectively. Intraperitoneal injections were of 150 ug of thymosin β4 in 300 ul PBS (or PBS only as a control) every three days starting from the day of ligation until the time of sacrifice for analysis, and another subset of mice received thymosin β4 through both intracardiac injection at the time of ligation as well as intraperitoneal injections as noted above. Other small pilot experiments involved delayed intraperitoneal administration of thymosin β4 and are discussed elsewhere (Chapter Three, Figure 8 & Discussion).

Analysis of cardiac function by echocardiography

Echocardiograms to assess systolic function were performed using M-mode and 2-dimensional measurements as described previously (Garner et al., 2003) and were analyzed for fractional shortening and ejection fraction, respectively. The measurements represented the average of six selected cardiac cycles from at least two separate scans performed in random-blind fashion with papillary muscles used as a point of reference for consistency in level of scan. End diastole was defined as the maximal left ventricle (LV) diastolic dimension and end systole was defined as the peak of posterior wall motion. Outliers in each experimental group were omitted for statistical analysis when groups had $n > 10$. Fractional shortening (FS), a surrogate of systolic function, was calculated from LV dimensions as follows: FS = EDD - ESD / EDD x 100%. Ejection fraction (EF) was calculated from two-dimensional images. EDD, end diastolic dimension; ESD, end systolic dimension.

Protein isolation and analysis

Protein was isolated from homogenized heart tissue using Trizol Reagent (Invitrogen # 15596-018) and standard Invitrogen protocols. The Bradford assay (Bio-Rad) was used to quantitate protein concentrations. Protein was then used for Western blotting with primary antibodies against ILK, Akt1, Akt1/2/3-P, Tβ4, VEGF, and GAPDH (all antibodies from Santa Cruz Biotechnology except Tβ4).

Calculation of scar volume

Scar volume was calculated using five or six sections through the heart of each mouse using Openlab 3.03 software (Improvision) similar to previously described (Balsam et al., 2004). Percent area of collagen deposition was measured on each section in blinded fashion and averaged for each mouse. Analyses shown here were done at 14 days for thymosin β4-treated hearts and at 42 and 63 days for SDF-1-treated hearts.

Immunohistochemistry

Embryonic or adult cardiac tissue was processed for immunolabeling experiments through one of three different methods. Tissue frozen after being taken through fixation with 4% paraformaldehyde or 10% formalin followed by 10% and 30% sucrose gradients was used for cryosectioning. Other hearts were embedded in paraffin after fixation in 4% paraformaldehyde or 10% formalin. A third group of hearts underwent methyl carnoy fixation (10% glacial acetic acid, 60% methanol, 30% chloroform) followed by 70% ethanol storage until embedding. Subsequent sectioning was done by Dr. Jim Richardson's Histology Core here at UT Southwestern Medical Center. Adult hearts were sectioned through at least ten equivalent levels from the base of the heart to the apex. Serial sections were used for trichrome sections and reaction with various antibodies.

Cryosections were used for immunofluorescence. Specifically, embryonic heart sections were incubated with anti-thymosin β4 (gift of H. Yin). Apoptosis in adult hearts was assayed using ProMega's DeadEnd Fluorometric TUNEL System (# G3250) or Intergen's ApopTag kit (# S7111); cell proliferation with antibody against H3B (Upstate Biotechnology, # 06-

570); angiogenesis with Factor VIII (Dako # A 0082); hematopoietic stem cells with c-kit (Santa Cruz, # sc-168); muscle actin with HHF35 (Dako # M0635).

Paraffin-embedded sections were used for radioactive RNA in situ hybridization; H&E staining for histology visualization; trichrome staining for scar tissue; PECAM staining (BD Biosciences, # 550274) for angiogenesis.

Methyl carnoy fixed sections were used for staining with isolectin B4 (Vector Labs, # B-1205) for angiogenesis. Quantitation was done by counting the number of vessels per 40x magnification field of view with five random fields near the area of infarction assayed for each mouse.

Statistical analyses

Statistical calculations were performed using t-test of variables (two-sample t-test assuming unequal variances) with 95% confidence intervals (Microsoft Excel 2003).

BIBLIOGRAPHY

(2002). "Cardiovascular Disease Statistics." from http://www.americanheart.org/presenter.jhtml?identifier=4478.

Abbott, J. D., Huang, Y., Liu, D., Hickey, R., Krause, D. S., and Giordano, F. J. (2004). Stromal cell-derived factor-1alpha plays a critical role in stem cell recruitment to the heart after myocardial infarction but is not sufficient to induce homing in the absence of injury. Circulation *110*, 3300-3305.

Adams, R. H., Diella, F., Hennig, S., Helmbacher, F., Deutsch, U., and Klein, R. (2001). The cytoplasmic domain of the ligand ephrinB2 is required for vascular morphogenesis but not cranial neural crest migration. Cell *104*, 57-69.

Aiuti, A., Webb, I. J., Bleul, C., Springer, T., and Gutierrez-Ramos, J. C. (1997). The chemokine SDF-1 is a chemoattractant for human CD34+ hematopoietic progenitor cells and provides a new mechanism to explain the mobilization of CD34+ progenitors to peripheral blood. J Exp Med *185*, 111-120.

Askari, A. T., Unzek, S., Popovic, Z. B., Goldman, C. K., Forudi, F., Kiedrowski, M., Rovner, A., Ellis, S. G., Thomas, J. D., DiCorleto, P. E.*, et al.* (2003). Effect of stromal-cell-derived factor 1 on stem-cell homing and tissue regeneration in ischaemic cardiomyopathy. Lancet *362*, 697-703.

Bajetto, A., Barbero, S., Bonavia, R., Piccioli, P., Pirani, P., Florio, T., and Schettini, G. (2001). Stromal cell-derived factor-1alpha induces astrocyte proliferation through the activation of extracellular signal-regulated kinases 1/2 pathway. J Neurochem *77*, 1226-1236.

Balsam, L. B., Wagers, A. J., Christensen, J. L., Kofidis, T., Weissman, I. L., and Robbins, R. C. (2004). Haematopoietic stem cells adopt mature haematopoietic fates in ischaemic myocardium. Nature *428*, 668-673.

Beltrami, A. P., Barlucchi, L., Torella, D., Baker, M., Limana, F., Chimenti, S., Kasahara, H., Rota, M., Musso, E., Urbanek, K.*, et al.* (2003). Adult cardiac stem cells are multipotent and support myocardial regeneration. Cell *114*, 763-776.

Bernanke, D. H., and Markwald, R. R. (1982). Migratory behavior of cardiac cushion tissue cells in a collagen-lattice culture system. Dev Biol *91*, 235-245.

Bhatia, G., Sosin, M., Leahy, J. F., Connolly, D. L., Davis, R. C., and Lip, G. Y. (2005). Hibernating myocardium in heart failure. Expert Rev Cardiovasc Ther *3*, 111-122.

Bleul, C. C., Fuhlbrigge, R. C., Casasnovas, J. M., Aiuti, A., and Springer, T. A. (1996). A highly efficacious lymphocyte chemoattractant, stromal cell-derived factor 1 (SDF-1). J Exp Med *184*, 1101-1109.

Bock-Marquette, I.*, Saxena, A.*, White, M. D., Dimaio, J. M., and Srivastava, D. (2004). Thymosin beta4 activates integrin-linked kinase and promotes cardiac cell migration, survival and cardiac repair. Nature *432*, 466-472.

Braunwald, E. (1997). Shattuck lecture--cardiovascular medicine at the turn of the millennium: triumphs, concerns, and opportunities. N Engl J Med *337*, 1360-1369.

Corcione, A., Ottonello, L., Tortolina, G., Facchetti, P., Airoldi, I., Guglielmino, R., Dadati, P., Truini, M., Sozzani, S., Dallegri, F., and Pistoia, V. (2000). Stromal cell-derived factor-1 as a chemoattractant for follicular center lymphoma B cells. J Natl Cancer Inst *92*, 628-635.

Cowan, C. A.*, Yokoyama, N.*, Saxena, A., Chumley, M. J., Silvany, R. E., Baker, L. A., Srivastava, D., and Henkemeyer, M. (2004). Ephrin-B2 reverse signaling is required for axon pathfinding and cardiac valve formation but not early vascular development. Dev Biol *271*, 263-271.

Damas, J. K., Eiken, H. G., Oie, E., Bjerkeli, V., Yndestad, A., Ueland, T., Tonnessen, T., Geiran, O. R., Aass, H., Simonsen, S.*, et al.* (2000). Myocardial expression of CC- and CXC-chemokines and their receptors in human end-stage heart failure. Cardiovasc Res *47*, 778-787.

Depre, C., and Vatner, S. F. (2005). Mechanisms of cell survival in myocardial hibernation. Trends Cardiovasc Med *15*, 101-110.

Doitsidou, M., Reichman-Fried, M., Stebler, J., Koprunner, M., Dorries, J., Meyer, D., Esguerra, C. V., Leung, T., and Raz, E. (2002). Guidance of primordial germ cell migration by the chemokine SDF-1. Cell *111*, 647-659.

Frohm, M., Gunne, H., Bergman, A. C., Agerberth, B., Bergman, T., Boman, A., Liden, S., Jornvall, H., and Boman, H. G. (1996). Biochemical and antibacterial analysis of human wound and blister fluid. Eur J Biochem *237*, 86-92.

Garner, L. B., Willis, M. S., Carlson, D. L., DiMaio, J. M., White, M. D., White, D. J., Adams, G. A. t., Horton, J. W., and Giroir, B. P. (2003). Macrophage migration inhibitory factor is a cardiac-derived myocardial depressant factor. Am J Physiol Heart Circ Physiol 285, H2500-2509.

Grant, D. S., Rose, W., Yaen, C., Goldstein, A., Martinez, J., and Kleinman, H. (1999). Thymosin beta4 enhances endothelial cell differentiation and angiogenesis. Angiogenesis *3*, 125-135.

Grove, J. E., Bruscia, E., and Krause, D. S. (2004). Plasticity of bone marrow-derived stem cells. Stem Cells *22*, 487-500.

Henkemeyer, M., Orioli, D., Henderson, J. T., Saxton, T. M., Roder, J., Pawson, T., and Klein, R. (1996). Nuk controls pathfinding of commissural axons in the mammalian central nervous system. Cell 86, 35-46.

Hood, A. E. (2005). Personal Communication. A. Saxena**:** Emergency medicine treatment post-myocardial infarction.

Huang, W. Q., and Wang, Q. R. (2001). Bone marrow endothelial cells secrete thymosin beta4 and AcSDKP. Exp Hematol *29*, 12-18.

Huff, T., Muller, C. S., Otto, A. M., Netzker, R., and Hannappel, E. (2001). beta-Thymosins, small acidic peptides with multiple functions. Int J Biochem Cell Biol *33*, 205-220.

Ismail, J. A., Poppa, V., Kemper, L. E., Scatena, M., Giachelli, C. M., Coffin, J. D., and Murry, C. E. (2003). Immunohistologic labeling of murine endothelium. Cardiovasc Pathol *12*, 82-90.

Jackson, K. A., Majka, S. M., Wang, H., Pocius, J., Hartley, C. J., Majesky, M. W., Entman, M. L., Michael, L. H., Hirschi, K. K., and Goodell, M. A. (2001). Regeneration of ischemic cardiac muscle and vascular endothelium by adult stem cells. J Clin Invest *107*, 1395-1402.

Jessup, M., and Brozena, S. (2003). Heart failure. N Engl J Med *348*, 2007-2018.

Kang, H. J., Kim, H. S., Zhang, S. Y., Park, K. W., Cho, H. J., Koo, B. K., Kim, Y. J., Soo Lee, D., Sohn, D. W., Han, K. S.*, et al.* (2004). Effects of intracoronary infusion of peripheral blood stem-cells mobilised with granulocyte-colony stimulating factor on left ventricular systolic function and restenosis after coronary stenting in myocardial infarction: the MAGIC cell randomised clinical trial. Lancet *363*, 751-756.

Kim, R. Y., Robertson, E. J., and Solloway, M. J. (2001). Bmp6 and Bmp7 are required for cushion formation and septation in the developing mouse heart. Dev Biol *235*, 449-466.

Kortesidis, A., Zannettino, A., Isenmann, S., Shi, S., Lapidot, T., and Gronthos, S. (2005). Stromal-derived factor-1 promotes the growth, survival, and development of human bone marrow stromal stem cells. Blood *105*, 3793-3801.

Loffredo, C. A. (2000). Epidemiology of cardiovascular malformations: prevalence and risk factors. Am J Med Genet *97*, 319-325.

Lu, Q., Sun, E. E., Klein, R. S., and Flanagan, J. G. (2001). Ephrin-B reverse signaling is mediated by a novel PDZ-RGS protein and selectively inhibits G protein-coupled chemoattraction. Cell *105*, 69-79.

Ma, J., Ge, J., Zhang, S., Sun, A., Shen, J., Chen, L., Wang, K., and Zou, Y. (2005). Time course of myocardial stromal cell-derived factor 1 expression and beneficial effects of intravenously administered bone marrow stem cells in rats with experimental myocardial infarction. Basic Res Cardiol *100*, 217-223.

Malinda, K. M., Sidhu, G. S., Mani, H., Banaudha, K., Maheshwari, R. K., Goldstein, A. L., and Kleinman, H. K. (1999). Thymosin beta4 accelerates wound healing. J Invest Dermatol *113*, 364-368.

Mangi, A. A., Noiseux, N., Kong, D., He, H., Rezvani, M., Ingwall, J. S., and Dzau, V. J. (2003). Mesenchymal stem cells modified with Akt prevent remodeling and restore performance of infarcted hearts. Nat Med *9*, 1195-1201.

Markwald, R. R., Fitzharris, T. P., and Manasek, F. J. (1977). Structural development of endocardial cushions. Am J Anat *148*, 85-119.

McGrath, K. E., Koniski, A. D., Maltby, K. M., McGann, J. K., and Palis, J. (1999). Embryonic expression and function of the chemokine SDF-1 and its receptor, CXCR4. Dev Biol *213*, 442-456.

Menasche, P., Hagege, A. A., Vilquin, J. T., Desnos, M., Abergel, E., Pouzet, B., Bel, A., Sarateanu, S., Scorsin, M., Schwartz, K.*, et al.* (2003). Autologous skeletal myoblast transplantation for severe postinfarction left ventricular dysfunction. J Am Coll Cardiol *41*, 1078-1083.

Mirshahi, F., Pourtau, J., Li, H., Muraine, M., Trochon, V., Legrand, E., Vannier, J., Soria, J., Vasse, M., and Soria, C. (2000). SDF-1 activity on microvascular endothelial cells: consequences on angiogenesis in in vitro and in vivo models. Thromb Res *99*, 587-594.

Murry, C. E., Soonpaa, M. H., Reinecke, H., Nakajima, H., Nakajima, H. O., Rubart, M., Pasumarthi, K. B., Virag, J. I., Bartelmez, S. H., Poppa, V., *et al.* (2004). Haematopoietic stem cells do not transdifferentiate into cardiac myocytes in myocardial infarcts. Nature *428*, 664-668.

Nagasawa, T., Hirota, S., Tachibana, K., Takakura, N., Nishikawa, S., Kitamura, Y., Yoshida, N., Kikutani, H., and Kishimoto, T. (1996). Defects of B-cell lymphopoiesis and bone-marrow myelopoiesis in mice lacking the CXC chemokine PBSF/SDF-1. Nature *382*, 635-638.

Nakagawa, O., Nakagawa, M., Richardson, J. A., Olson, E. N., and Srivastava, D. (1999). HRT1, HRT2, and HRT3: a new subclass of bHLH transcription factors marking specific cardiac, somitic, and pharyngeal arch segments. Dev Biol 216, 72-84.

Neuhaus, T., Lutz, C., Stier, S., Totzke, G., Gruenewald, E., Fronhoffs, S., Sachinidis, A., Vetter, H., and Ko, Y. D. (2003). The use of suppression subtractive hybridization for the study of SDF-1alpha induced gene-expression in human endothelial cells. Mol Cell Probes *17*, 245-252.

Olson, E. N., and Srivastava, D. (1996). Molecular pathways controlling heart development. Science *272*, 671-676.

Orimo, A., Gupta, P. B., Sgroi, D. C., Arenzana-Seisdedos, F., Delaunay, T., Naeem, R., Carey, V. J., Richardson, A. L., and Weinberg, R. A. (2005). Stromal fibroblasts present in invasive human breast carcinomas promote tumor growth and angiogenesis through elevated SDF-1/CXCL12 secretion. Cell *121*, 335-348.

Orlic, D., Kajstura, J., Chimenti, S., Jakoniuk, I., Anderson, S. M., Li, B., Pickel, J., McKay, R., Nadal-Ginard, B., Bodine, D. M., *et al.* (2001). Bone marrow cells regenerate infarcted myocardium. Nature *410*, 701-705.

Palmer, A., and Klein, R. (2003). Multiple roles of ephrins in morphogenesis, neuronal networking, and brain function. Genes Dev *17*, 1429-1450.

Pillarisetti, K., and Gupta, S. K. (2001). Cloning and relative expression analysis of rat stromal cell derived factor-1 (SDF-1)1: SDF-1 alpha mRNA is selectively induced in rat model of myocardial infarction. Inflammation *25*, 293-300.

Porcile, C., Bajetto, A., Barbieri, F., Barbero, S., Bonavia, R., Biglieri, M., Pirani, P., Florio, T., and Schettini, G. (2005). Stromal cell-derived factor-1alpha (SDF-1alpha/CXCL12) stimulates ovarian cancer cell growth through the EGF receptor transactivation. Exp Cell Res *308*, 241-253.

Runyan, R. B., and Markwald, R. R. (1983). Invasion of mesenchyme into three-dimensional collagen gels: a regional and temporal analysis of interaction in embryonic heart tissue. Dev Biol *95*, 108-114.

Safer, D., Elzinga, M., and Nachmias, V. T. (1991). Thymosin beta 4 and Fx, an actin-sequestering peptide, are indistinguishable. J Biol Chem *266*, 4029-4032.

Schmucker, D., and Zipursky, S. L. (2001). Signaling downstream of Eph receptors and ephrin ligands. Cell *105*, 701-704.

Sosne, G., Szliter, E. A., Barrett, R., Kernacki, K. A., Kleinman, H., and Hazlett, L. D. (2002). Thymosin beta 4 promotes corneal wound healing and decreases inflammation in vivo following alkali injury. Exp Eye Res *74*, 293-299.

Srivastava, D., and Olson, E. N. (2000). A genetic blueprint for cardiac development. Nature *407*, 221-226.

Sugi, Y., Yamamura, H., Okagawa, H., and Markwald, R. R. (2004). Bone morphogenetic protein-2 can mediate myocardial regulation of atrioventricular cushion mesenchymal cell formation in mice. Dev Biol *269*, 505-518.

Sun, H. Q., Kwiatkowska, K., and Yin, H. L. (1996). beta-Thymosins are not simple actin monomer buffering proteins. Insights from overexpression studies. J Biol Chem *271*, 9223-9230.

Tachibana, K., Hirota, S., Iizasa, H., Yoshida, H., Kawabata, K., Kataoka, Y., Kitamura, Y., Matsushima, K., Yoshida, N., Nishikawa, S.*, et al.* (1998). The chemokine receptor CXCR4 is essential for vascularization of the gastrointestinal tract. Nature *393*, 591-594.

van den Hoff, M. J., Moorman, A. F., Ruijter, J. M., Lamers, W. H., Bennington, R. W., Markwald, R. R., and Wessels, A. (1999). Myocardialization of the cardiac outflow tract. Dev Biol *212*, 477-490.

Vlahakis, S. R., Villasis-Keever, A., Gomez, T., Vanegas, M., Vlahakis, N., and Paya, C. V. (2002). G protein-coupled chemokine receptors induce both survival and apoptotic signaling pathways. J Immunol *169*, 5546-5554.

Wang, H. U., Chen, Z. F., and Anderson, D. J. (1998). Molecular distinction and angiogenic interaction between embryonic arteries and veins revealed by ephrin-B2 and its receptor Eph-B4. Cell *93*, 741-753.

Wunsch, A. M., Little, C. D., and Markwald, R. R. (1994). Cardiac endothelial heterogeneity defines valvular development as demonstrated by the diverse expression of JB3, an antigen of the endocardial cushion tissue. Dev Biol *165*, 585-601.

Yamagishi, H., Maeda, J., Hu, T., McAnally, J., Conway, S. J., Kume, T., Meyers, E. N., Yamagishi, C., and Srivastava, D. (2003). Tbx1 is regulated by tissue-specific forkhead proteins through a common Sonic hedgehog-responsive enhancer. Genes Dev 17, 269-281.

Yamagishi, T., Nakajima, Y., Miyazono, K., and Nakamura, H. (1999). Bone morphogenetic protein-2 acts synergistically with transforming growth factor-beta3 during endothelial-mesenchymal transformation in the developing chick heart. J Cell Physiol *180*, 35-45.

Yu, F. X., Lin, S. C., Morrison-Bogorad, M., Atkinson, M. A., and Yin, H. L. (1993). Thymosin beta 10 and thymosin beta 4 are both actin monomer sequestering proteins. J Biol Chem 268, 502-509.

Zou, W., Machelon, V., Coulomb-L'Hermin, A., Borvak, J., Nome, F., Isaeva, T., Wei, S., Krzysiek, R., Durand-Gasselin, I., Gordon, A.*, et al.* (2001). Stromal-derived factor-1 in human tumors recruits and alters the function of plasmacytoid precursor dendritic cells. Nat Med *7*, 1339-1346.

Zou, Y. R., Kottmann, A. H., Kuroda, M., Taniuchi, I., and Littman, D. R. (1998). Function of the chemokine receptor CXCR4 in haematopoiesis and in cerebellar development. Nature *393*, 595-599.

VITAE

Ankur Saxena was born in Troy, Michigan, just outside Detroit, on February 11, 1978 to Dr. Ravi N. Saxena and Mrs. Alka Saxena. Moving extensively during his childhood, including a stint overseas, Ankur eventually graduated in 1996 from Clements High School in Sugar Land, TX. He then attended the University of Texas at Austin, where he spent three years before graduating in July 1999 with a Bachelor of Science in Molecular Biology, a minor in Spanish, and the lifelong ability to bleed burnt orange. In August 1999, Ankur entered the Graduate School of Biomedical Sciences at the University of Texas Southwestern Medical Center at Dallas and joined the lab of Dr. Deepak Srivastava in May 2000. While there, Ankur studied the functions of signaling molecules in the heart by day and doubled as a masked crusader superhero by night. The latter nocturnal exploits are unfortunately outside the scope of this vitae in addition to being classified by the federal government.

Permanent Address: 4507 Summer Lakes
Sugar Land, TX 77479